

Synthesis of deep multichannel seismic and high resolution sparker data: Implications for the geological environment of KG offshore, Eastern Continental Margin of India

M.V. Ramana^{a,b*}, Anitha. G^a, Maria Desa^a, T. Ramprasad^a, Pawan Dewangan^a

^a CSIR-National Institute of Oceanography, Dona Paula, Goa 403 004, India

^b Mauritius Oceanography Institute, Victoria Avenue 230 427 4434, Mauritius

*Corresponding author (email: mangipudi1950@gmail.com, phone: 00230 57827280)

Abstract

Proven hydrocarbon occurrence in the Krishna Godavari (KG) basin, a part of the Eastern Continental Margin of India initiated intense exploration activities to discern the potential hydrocarbon bearing structures/payoff zones. Recent discovery of gas hydrates in its offshore triggered detailed exploration measures adopting advanced seismic data acquisition techniques supported by deep drilling to understand its genesis. Interpretation of Multichannel Seismic (MCS) sections highlighted several distinct horizons from Lower Cretaceous to Recent in the sediment overburden, and the nature and configuration of the underlying crust. The sections also depicted the presence of growth faults, shale bulging, toe thrust faulting, delta progradation, active sliding/slumping, buried channels, pinchout structures and reflection free zones, indicating the different types of sedimentary processes, varied geological environments and neotectonic activity in the KG offshore. High resolution sparker (HRS) data revealed subsidence, gas/fluid expulsion pathways, occasional diapiric intrusions and growth faulting in the upper slope, and toe thrust faulting, upthrust and diapiric intrusions in the lower slope. The mid slope is characterised by a well stratified E-W trending basin bounded by upthrust and diapirism. The entire region is associated with gas escape features (blanking zones, columnar type gas vents, fault controlled mud/shale diapirs, large dimension gas saturated zones and pockmarks). The growth faults, shale bulging and toe thrusting seen in the MCS data since Oligocene time could be linked to shale diapirism, upthrust, gas/fluid expulsion, subsidence and mini-basin formation observed on the shallow HRS records. Synthesis of these datasets suggests that the distribution of gas hydrate in the shallow sediments may be controlled by the deeper structural and tectonic configuration. Therefore, knowledge about shallow sedimentary column and its connectivity with deeper strata through faults/fractures and other structural features, and the geological architecture are significantly important to evaluate the genesis of gas hydrates.

Key words: KG offshore, gas hydrate, high resolution seismic reflection sparker data, high quality multichannel seismic data, deep seated faults, gas upthrust, mud diapirism

1. Introduction

Krishna-Godavari (KG) offshore basin (Fig.1) drew the attention of oil majors due to its proven hydrocarbon potential over the past two and half decades. Persistent demand for oil and natural gas compelled the Ministry of Petroleum and Natural Gas, Government of India to search for an alternative to the conventional hydrocarbons. Gas hydrate, a consolidated form of pure methane gas could be a suitable substitute, if detected along the Indian offshore. These gas hydrate deposits are found to occur in marine slope sediments and permafrost regions, where low temperatures, high pressures and sufficient organic carbon are found (Kvenvolden, 1993). Several researchers used multichannel seismic reflection (MCS) data to infer gas hydrate occurrence by mapping bottom simulating reflector (BSR, an anomalous seismic reflector, and a gas hydrate related proxy) that represents the base of gas hydrate stability zone (Shipley et al., 1979; Kvenvolden, 1998; Hyndman et al., 1992). The gas hydrate fields of McKenzie Delta, Nankai Trough, Blake Ridge and Hydrate Ridge are the best known examples inferred using BSRs (Holbrook, 2001; Suess et al., 2001; Nouze et al., 2004; Dallimore and Collett, 2005).

The resource map of India (NIO, 1997) in conjunction with the inferred BSRs (NIO, 2001) suggested the likely occurrence of gas hydrates along the continental margins of India. Multidisciplinary investigations in the KG offshore (NIO, 2003), together with seismic results aided in selecting suitable locations for ground truthing. The subsequent drilling program onboard JOIDES Resolution confirmed the presence of a fully developed gas hydrate system in the KG and Mahanadi offshore areas, and the Andaman Sea under varied tectonic (passive and active margin) regimes/settings (Collett et al., 2008). Gas hydrate deposits are known to occur in different forms, i.e., disseminated, nodular, layered, massive (Sloan, 1990). The KG offshore is known for the occurrence of gas hydrate in fractures (Riedel et al., 2010) as well as in sand bearing beds (Riedel et al., 2011). The thickness of these hydrate zones varies from a few centimetres to few meters with an exception of one or two locations, where the thickness is >100 m.

It is important to understand the subsurface geological environment, architecture of the upper and deeper sediments, associated structural elements and the basement configuration to infer the genesis and distribution of gas hydrates in a particular region. The conventional MCS data, though insufficient to estimate the potential of gas hydrates due to their unknown nature and lateral extent, can provide the complete architecture of the sediment column and acoustic basement. The High Resolution Sparker (HRS) system can detect fine scale structures as thin as 1-2 m within the upper few hundred meters sedimentary column. Since gas hydrates occur within the upper few hundred

meters, the HRS system forms a powerful tool for its exploration. Integration and combined interpretation of the conventional MCS and HRS data is of utmost importance to link the shallow gas hydrate related structures to the characteristics of the deeper sediment overburden and underlying crust. To that extent, we have used the processed MCS sections (GXT-1, GXT-2, AD-1, AD-2 and AD-3) and HRS data in the present study to decipher the subsurface geology and relate the shallow structures to the deeper structural configuration. The HRS data in the KG offshore basin depicted the presence of several gas escape features, while the MCS data defined major geological boundaries, deeper sources of the shallow disturbances and growth faults extending up to Eocene.

2. Geological setting

The Eastern Continental Margin of India resulted due to the breakup of India from the contiguous Australia-Antarctica in the Early Cretaceous, and subsequent dispersion of the continents in time and space (Ramana et al., 1994). The Eastern Margin includes the Bengal and Mahanadi Basins in the north, and Krishna-Godavari (KG) and Cauvery Basins in the south, all petroliferous in nature. The onshore pericratonic KG Basin, in existence since the Jurassic, extends offshore beyond mid-slope (Rao, 2001; Sahu, 2005; Gupta, 2006). This basin extends between Kakinada in the north and Ongole in the south, and occupies an area of ~28000 and ~145000 sq. km on land and offshore respectively (Rao, 2001; Bastia, 2007). Some of the ~NE-SW trending horst and graben like onshore structures are seen extending offshore (Fig. 1). The lower slope region and further offshore is filled with the Cretaceous-Recent sediments (Curry et al., 1982; Pateria et al., 1992).

The onshore grabens filled with 3-6 km thick volcanic lava flows are intercalated with intertrappean clay, limestone and sand beds (Rao and Mani, 1993; Rao, 2001; Sahu, 2005). The offshore basin is comprised predominantly of claystone with sand and siltstone beds, with the basement overlain by the lower Cretaceous and Paleocene shales with intertrappean Razole volcanic flows (Rao and Mani, 1993; Rao, 2001; Sahu, 2005; Gupta, 2006). The Eocene Vadaparru shale, thin Oligocene claystone, Miocene-early Pliocene Ravva sandstone formations and Godavari clay of Pleistocene to Recent are the geological successions resting on the top of Paleocene (Rao, 2001; Bastia and Nayak, 2006; Bastia et al., 2006).

The shelf is very narrow at the mouth of river Krishna influencing sediment dispersal pattern over time. The Krishna delta is river dominated with more sand content due to erosion of peninsular gneiss and Cuddapah basin, composed of metamorphic and metasedimentary rocks of Archean and Proterozoic ages respectively (Sastri et al., 1981). The Godavari River forms a wave dominated delta over a wider shelf, draining the Deccan volcanics and Archean Eastern Ghats depositing sediments

with mixed clay and sand rich character. The huge sediment influx encouraged the development of growth fault activity in the shelf, capturing the shale load within the accommodation space created (Choudhuri et al., 2010).

Sedimentological analysis revealed that the shallow sediments in the KG offshore are dominantly comprised of nannofossil rich clays with occasional incursions of ~10-20 m thick foraminifera bearing clay zones and carbonate/pyrite bands with authigenic carbonates (Collett et al., 2008). Several researchers reported different sedimentation rates for the KG offshore. For example: a sedimentation rate of 1.06 m/Ky (Raju et al., 1994) was reported for the shelf environment, while variable sedimentation rates ranging from 0.07 to 0.125 m/Ky were reported (Rao and Mani, 1993) for the upper Cretaceous to Miocene strata. The sedimentary cycles of the NGHP-01 expedition cores tentatively indicated an average sedimentation rate of 0.15 m/Ky (Collett et al., 2008) for the upper few hundred meter sediments. A recent study of 30 m long core in the KG offshore indicated higher sedimentation rates of 2.483 to 0.86 m/Ky for the upper 5 to 6 m, and 0.175 m/Ky for the rest of the core length (Mazumdar et al., 2009). Highly variable pre- and Holocene sedimentation rates have been inferred based on dating of additional long cores (Mazumdar et al., 2012).

3. Data and Methodology

About 500 line km of high resolution seismic reflection (HRS) data acquired with a 10 Kilo Joule Sparker system and about 90 km industry acquired MCS data have been used in the present study (Fig. 2). To understand the deep sedimentary structure and basement configuration, we have used two India-Span deep seismic reflection profiles acquired by GX Technology (provided by Directorate General of Hydrocarbons (DGH)) totalling ~300 line km in vicinity of the study area (Fig. 2). The GXT-1 profile lies within the study area off the Godavari river mouth with the oil industry drill well at its northwestern end, while the GXT-2 profile originates off the Krishna river mouth. Major horizons were identified on the seismic data and ages were assigned using the drill well information and previous literature (Curry et al., 1982; Pateria et al., 1992; Choudhuri et al., 2010; Mandal et al., 2014). The HRS data has been primarily used to decipher the finer details of the upper sedimentary strata, while the MCS data to decipher the macro/microstructures within the entire sedimentary column. An integrated analysis of these datasets has been made to infer the link between the deeper and shallow geological environments, and to map the different structures which may act as gas/ fluids migration pathways that control the gas hydrates accumulation zones within the upper shallow strata. Further an attempt was made to understand the depositional history of the study area.

4. Results

Interpretation of HRS data:

The HRS data provides detailed information about the few hundred meters below the seabed. Interpretation of the HRS data along the dip lines (Fig. 2 & 3) shows a maximum penetration of ~650 ms TWT (~520 m) below the seabed and well defined lithological boundaries within the sediments with a vertical resolution of ~2 m. The data covers the area between the water depths of 467 ms (~350 m) in the upper slope and 2133 ms (~1600 m) in the lower slope region with an average gradient of 1:37 (Fig. 3). The upper slope region is intruded by 2.0-4.0 km wide features (Fig. 3) with a relief of 30 to 80 ms. The lower-slope is more undulatory as compared to upper or mid slope, and is characterized by 1.5-2.5 km wide positive topographic features with subsurface folding. The relief of these positive features varies from 40-100 ms (32-80 m) from the adjacent seafloor topography.

The HRS sections allowed definition of nine distinct reflectors below the mid-slope and about four in the upper and lower slope regions. A strong erosional surface below the seabed overlain by distinct layering pattern is interpreted as the Last Glacial Maximum (LGM) surface. The sediment load over this surface is maximum in the mid slope (~140 ms) and is minimum in the upper and lower slope regions (Fig. 3).

The upper slope region is mainly associated with intense faulting and occasional presence of diapirism/gas upthrust (Fig. 3). These faults are acting as paths for gas/fluid expulsions. The subsurface of the upper slope is also seen associated with cut and fill type channels (Fig. 3d) and blanking zones with variable widths (0.4-0.8 km). A channel like feature (between shots 5300 and 5500) exists on the upper mid slope region, and the pattern of horizons associated with this feature suggests that it could be a depression/minibasin rather than a paleochannel, and might have evolved due to neotectonic activity/disturbances caused by gas upthrust/diapirism (Fig. 3d(i)). A fault controlled subsidence (between shots 4400 and 5300) resulting in a graben like structure is also conspicuous in the upper slope region (Fig. 3d & 4b), and is characterised by a number of parallel to sub-parallel reflectors. Gas up-thrust from deep along the pre-existing faults created the shoulders of the graben (Fig. 3d). Unlike the upper slope sediments, the mid slope sediment pack is characterised by 6 to 9 dipping reflectors with a thickness of 650 ms TWT. This dipping sediment pack belongs to a basin trending in an ~E-W direction with variable dimensions both laterally and vertically (Fig. 3 & 4a). This slope basin shallows towards the east, i.e.. ~168 ms along line L4 (Fig. 3d) beyond which it is absent (Fig. 3e & f). The sediments within the basin are least distorted by faults (Fig. 3a).

The basin edge towards the lower slope is seen associated either with gas upthrust or diapiric intrusion (Fig. 3). The presence of pockmarks (Fig. 3g) on the seabed at the edge of the slope basin confirms the active process of gas/fluid expulsion. The layering pattern also changes from the end of the mid slope to lower-slope i.e., absence of internal reflections, and less number of reflectors. The lower slope region having irregular topography is seen severely folded up to the seabed. The subsurface strata depict the presence of gas saturated columnar zones sandwiched between mud diapirs (Fig. 3).

The shallow subsurface geology (up to 200 m) has been inferred by correlating the prominent reflectors (Fig. 3) with that of the lithology derived from the sedimentological analysis of the core at site NGHP-01-05 (Collett et al., 2008). The acoustically transparent zones in the seismic records represent the nannofossil-bearing clays, while the high reflective zones coincide with the nannofossil-rich clay. The HRS sections show several reflectors below the described core length of the NGHP site (200 mbsf). Thus the impedance contrast within the sediments may be due to the variation in the lithology.

Interpretation of MCS data:

The fine scale structures and associated stratification of the study area have been discussed using interpretation of HRS data, while the MCS data (Fig. 4 & 5) has been used to infer the deeper geological events. Interpretation of GXT sections (Fig. 5) reveals the presence of a prominent, highly undulatory and severely faulted deep reflector corresponding to the basement. Along the line GXT-1 (Fig. 5a), the basement occurs between 7.5 and 9 s TWT in the slope region and further offshore, while along the line GXT-2 (Fig. 5b), the basement occurs at varying depths from the shelf to deep offshore, i.e., 3.5 s TWT below the shelf, between 4 and 5.5 s in the slope region and up to 9 s towards deep offshore. Along line GXT-2, a strong reflector occurring below the basement at a maximum depth of 11 s TWT (Fig. 5b) and shallowing to 9 s towards offshore has been interpreted as the Moho. In the slope region, between shots 1500 and 1800, the Moho is interrupted and deeply originated intrusive bodies are seen as reflection free zones causing significant relief to the basement. Between shots 2700 and 2950, the Moho reflector is discontinuous and undulatory, while between shots 3100 and 3300, it reaches up to the basement. Here the basement reflector is weak and no clear basement sediment interface is observed. Beyond this zone, the Moho is seen at deeper depths (~10.5 s). Along line GXT-1, no Moho reflector is observed, but between shots 6000 and 6500, the basement reflector is very weak, as a result the basement-sediment interface is not clearly deciphered (Fig. 5a). The reflection free zone with weak basement reflector can be considered akin to mantle

unroofing belonging to proto-oceanic crust reported elsewhere. Based on the disposition of the basement and underlying Moho, the basement can be differentiated into three types of crust, i) continental crust ii) proto-oceanic crust and iii) oceanic crust.

The basement is overlain with 3- 4 s TWT thick sediments below the shelf (Fig. 5b) and ~ 7 s in the slope region (Fig. 5a). Based on the seismic reflection characteristics, the sediment overburden over the basement has been divided into 6 sequences and their tops have been designated as H1 to H6 (Fig. 5). From the previous literature (Curry et al., 1982; Pateria et al., 1992; Choudhuri et al., 2010) and oil industry drill well information, we have assigned ages to these major sequences. The sequence immediately over the basement is inferred as lower Cretaceous and its top has been marked as H1. This sequence is characterised by medium to low amplitude and chaotic reflection pattern. The horizon above H1 is marked as H2 and sedimentary pack between H1 and H2 depicting parallel continuous, high to medium amplitude reflection pattern is inferred as the upper Cretaceous sequence. These Cretaceous sediments are also seen below the shelf and the slope region between basement highs (Fig. 5b).

The unconformity above H2 corresponds to the Top of Eocene (H3). Within the Paleocene-Eocene sedimentary pack i.e., between H3 and H2, a 0.5 s TWT thick semi transparent reflection zone is seen from shot 1950 which pinches out at shot 2800 (Fig. 5b). This wedge out like feature may correspond to Paleocene clay deposits. The stratum immediately over this pinchout structure (from shots 1900 to 2700) consisting of wavy reflections may correspond to silt and sand mix. Between shots 1450 and 1950, growth faulting and thrusting is seen up to the wedge out feature. The undisturbed top of Eocene horizon over the inferred basement highs between shots 1400 and 1900 suggests that these highs may have been emplaced prior to Eocene. Within the depressions formed by these basement highs, the sagging reflection pattern is that of a mini-basin, while the pondfill pattern (shots 1250 to 1350) is that of a channel. Along the line GXT-1 (Fig. 5a), the Paleocene-Eocene pack (between H2 and H3) is nearly parallel and of low amplitude reflections towards offshore but depicts distorted nature with high to medium amplitude reflections in the slope region (between shots 7890 and 8690). This distorted nature appears as rotated blocks indicating severe faulting, deformation and thrusting.

Another significant horizon H4 represents top of Oligocene overlying a thin (<1 s) semitransparent to chaotic, low to medium amplitude and undulatory sediment sequence of Oligocene period. The upper Oligocene sequence appears heavily disturbed in the slope region along profile GXT-2. Growth faulting continues at shot 1500 and gravity sliding occurs at shelf and slope,

with minor thrusting at lower slope (between shots 1500 and 1800; Fig. 5b). The Oligocene pack is associated with bulging at the upper and mid slope region and toe thrust faulting at lower slope (GXT-1; Fig. 5c).

The prominent horizon 'H5' corresponds to top of Miocene. The thickness of the Miocene sedimentary pack is varying between 0.6 s and 2.5 s TWT from shelf to deep offshore side. This pack consisting of continuous, parallel and strong reflections onlaps the strong erosional surface of Oligocene top 'H4' (Fig. 5a & b). Towards deep offshore, ~0.5 s thick semi transparent pack is seen within this Miocene sequence indicating mass transport deposition. Along profile GXT-1, this Miocene pack is characterised with growth faulting and thrusting in the upper slope (Fig. 5a & c), whereas it is associated with shale bulging and toe thrust faulting from mid to lower slope. Along profile GXT-2, this pack is not discernible in the slope region (Fig. 5b). Further, this Miocene pack is overlain by the Pliocene sediments which depict parallel to sub-parallel continuous reflections of low to medium amplitude. The top of this sequence H6 represents the Plio-Pleistocene boundary. Towards offshore, a series of mass transport deposits are seen as semi transparent reflections in the Pliocene to Pleistocene time. The horizon H6 occurs at ~0.5 s below the seabed towards offshore. The Pleistocene to Recent pack is maximum on the shelf (~1.5 s along GXT-1 and 0.8 s along GXT-2; Fig. 5a & b). Delta progradation with growth faulting is seen along profile GXT-2 (Fig. 5d) initiated prior to Pleistocene time.

Along the line GXT-2, establishing the continuity of the seismic horizons from Oligocene top to Recent between shots 1580 and 1800 is rather difficult due to the observed severely disturbed and chaotic reflection patterns. These patterns belong to a slumping structure occurring over a length of ~14 km in the mid and lower slope regions, and is associated with several active faults (Fig. 5e). This region is also characterised by deep seated faults from the Cretaceous basement to the seabed, and deeply originated intrusive bodies which emplaced prior to Eocene time. The slumping is probably due to slope instability which resulted due to fluid expulsion, high sedimentation rates and/or recent/paleo tectonics.

The sections AD-1, AD-2 & AD-3 (Fig. 4) depict ~5 s TWT information in the upper to lower slope region. Using the GXT profiles, the major geological boundaries (H3- Top of Eocene; H4 - Top of Oligocene; H5 – Top of Miocene and H6- Plio-Pleistocene boundary) are inferred on these profiles. The top of Eocene (H3) is associated with severe faulting and folding/doming between the upper slope and beginning of mid slope. This domal appearance is seen in the Miocene and Pliocene sequences too. The mid slope basin, interpreted from the HRS data is prominently seen on

the top of H6 bounded with faulting and/or upthrust (Fig. 4), while it is absent towards northeast (Fig. 4c). The underlying Plio-Miocene sequences also depict the basin related sagging effect between the bulging and folding.

Growth faulting, thrusting and mass transport deposits are also seen within the Miocene sequence. The Pliocene sequence between H5 and H6 is associated with pull-up and pinchout structures (AD-2; Fig. 4b). This velocity pull-up signature (anticline shape) suggests the effect of upwelling of the Miocene bed up to the Pleistocene. The chaotic and hummocky reflections within this sequence may indicate the presence of turbidity and mass transport deposits of Pliocene age. BSRs were identified along these profiles suggesting the likely presence of gas hydrate around the slope basin (Fig. 4). The Plio-Pleistocene boundary (H6) on the seismic records coincides with the bottom most reflector in the mid slope region on the HRS sections (Fig. 3b & h).

5. Discussion

The present study suggests that the basement of KG offshore is associated with three different types of crust i) continental crust, ii) proto-oceanic crust and iii) oceanic crust (Fig. 5a & b). A similar crustal scenario has been inferred by Nemcok et al., (2012) in this region. The KG offshore region has a very narrow shelf (<30 km). The rifted basement is discontinuous due to normal faulting, while the basement highs may be due to sporadic volcanic activity (Fig. 5). The synrift/post-rift sediments fill the relief of the oceanic crust terminating against the steep slopes of these highs. Six major seismic sequences have been inferred in the sediment overburden ranging from Cretaceous to Recent. Normal basinal sedimentation prevailed in this region up to Cretaceous time, with little tectonic activity. In Paleogene time, excess sedimentation resulted in growth faulting and thrusting as seen in the seismic sections (Fig. 5). This tectonics continued even up to Miocene time and resulted in shale bulging from Oligocene to Recent.

The HRS sections depict shallowing and undulations in the upper and lower slope regions due to the intense diapiric activity (vertical compression) associated with gas upthrust. The mid-slope region has a well stratified basin and is least effected by either the gas/fluid expulsions or subsurface faulting/folding, indicating the prevalence of low energy environment (Fig. 3). The bottom most reflector in the mid slope region has been inferred as the Plio-Pleistocene boundary under seismic constraints (Fig. 3b & h). Based on the inferred LGM surface, the sediments above it appear to be deposited with sedimentation rates of ~3 m/Ky and ~5 m/Ky in the upper and middle slope regions respectively, while the rates are negligible in the lower slope region and beyond. The deeper

sediments between the LGM and Plio-Pleistocene boundary may have been deposited with the sedimentation rate of up to 0.1 m/Ky in the mid slope region.

The interpreted sections of HRS and MCS data depict the presence of growth faults, toe thrust faults, anticlines, fault controlled basin, folded/domal shaped structures, turbidite flows, mass transport deposits, cut and fill type channels, and velocity pull-up structure. The mud diapirs, blanking zones, pinchouts, pockmarks, diapirs, gas upthrusts and columnar type gas saturated zones are some of the other typical features inferred in the present study. Similar features have been reported in the KG offshore and attributed to shale tectonics and intense faulting (Bastia and Nayak., 2006; Bastia et al., 2006; Ramana et al., 2006, 2009; Shanmugam, 2009; Shanmugam et al., 2009; Ramprasad et al., 2011; Dewangan et al., 2010; 2011).

The gas upthrust features widespread in the upper mid and lower slope regions extend upwards through faults/folds affecting not only the Miocene horizons but also the upper Plio-Pleistocene sequences (Anitha et al., 2014; Fig. 4). The manifestation of these gas upthrusts on the seafloor is seen in the form of gas vents and pockmarks (Fig. 3). The long wavelength folded seafloor topography in the lower slope region overlies the strata that are folded due to huge columnar type gas saturated zones/gas upthrust features. This folding is the resultant of deep seated diapirism and upward migration of fluids/gas through fault zones due to enormous pressure below. This folding probably belongs to the proximal bulge of Miocene-Pliocene age inferred by Choudhuri et al., (2010). The MCS data suggest that these features appear to be emanated from deeper horizons i.e., up to Paleocene time and are the manifestation of shale tectonism/mud diapirism. Choudhuri et al., (2010) suggested that shales of Paleocene-Eocene in the deeper shelf and upper slope areas moved as a series of thrust slices, whereas the younger Miocene-Pliocene shales moved as individual bulges. They inferred linkages between sediment depocenters, growth faults, mobile shales, lithological variability and tectonic conditions. A similar scenario is seen in the present study with individual diapirism of Mio-Pliocene age originating due to the deep toe thrusting right from Paleocene-Eocene (Fig. 3 to 5).

Excessive formation pressures and shale tectonism/mud diapirism have been reported in the KG offshore basin (Rao and Mani, 1993; Satyanarayana et al., 1996; Sahu, 2005; Bastia et al., 2006; Chatterjee, et al., 2010). Similar conditions can be inferred based on the observed broad wavelength bulging and folded/domal shaped structures since Miocene period (Fig. 4 & 5). Instances of neotectonic activity are reported in the Eastern Continental Margin of India (Rao and Mani, 1993; Chatterjee et al., 2010). Marine geophysical studies (Murthy et al., 2010) inferred moderate

seismicity associated with land–ocean tectonic elements along the eastern offshore. The tectonic setting of the East Coast of India with predominant W–E and NW–SE lineaments/fracture system resulted in a basinal to non-basinal mosaic suggesting its vulnerability to neotectonic activity. Therefore, some of the observed features on the HRS sections are the manifestation of the combined effect of the gas upthrusting due to excessive pressures and neotectonic activity.

A schematic representation of the deposition history of the entire sedimentary column indicates that all the shallow disturbances have deep seated roots (Fig. 6). High sedimentation rates during Paleocene-Eocene resulted in shelfal instability leading to the formation of growth faults and series of toe thrusts. Further continued sediment influx in the Oligocene resulted in delta progradation, gravity sliding, thrusting and shale bulging (Fig. 5). Intense sedimentation occurred in the Miocene due to the combined influx from the Krishna and Godavari rivers and the Bengal Fan (Curry et al., 1982; Fig. 5). This excessive load caused faulting and extension resulting in low degree long wavelength folding and shale bulging (Fig. 5c). Further, faster burial prevented the escape of fluids/gases from the lower layers causing increase in pore pressure destabilizing the sediment sequences. Growth faulting and toe thrusting continued up to Recent times with individual shale diapirism, upthrusting and upward migration of gas/fluids.

Recent drilling in the KG offshore basin showed the presence of thick accumulation of gas hydrate deposits in the fractures (Riedel et al., 2010), therefore the inferred fractures/faults are significant in assessing the gas hydrate potential of this area. Deep seated faults have been inferred in this study and these faults act as pathways for the upward migration of the gas/fluids from below. Gas hydrate deposits found in the KG offshore are probably controlled by the deeper structural and tectonic configuration, and the migration of the gas/gas bearing fluids from deep through these faults.

6. Conclusions

HRS data reveals that the upper slope is mainly characterised by a zone of subsidence, gas/fluid expulsion path ways, occasional diapiric intrusions and growth faulting. The mid slope is associated with a slope basin of low energy environment, bounded by gas/fluid expulsion zones towards upper slope and diapirism/toe thrusting towards lower slope. The sediments below the upper-mid slope region are severely faulted, and the strata attain domal shape (anticline like structure) with considerable wave lengths. The lower slope is characterised by intense faulting, upthrust and diapiric intrusions. The observed long wavelength undulations in the lower slope region are the manifestation of deep seated shale tectonism/ neotectonic activity. The entire region is

associated with gas escape features (blanking zones, columnar type gas vents, fault controlled mud/shale diapirs, large dimension gas saturated zones and surface mounds).

MCS data facilitated the mapping of six major sediment sequences from the Cretaceous to Recent. Sediment sequences of Paleocene-Eocene time depict series of thrusting and growth faulting probably due to rapid sedimentation. This led to shale bulging in the Oligocene period. Continued fast sedimentation in the Miocene resulted in rigorous faulting, thrusting leading to individual shale diapirism/bulging seen in the younger Pliocene to Recent sediments. In the Krishna Offshore, the 14 km wide slumping/sliding structure and active growth faulting at the shelf break depicts the present day slope instability, while the Godavari Offshore is characterised by shale bulging and toe thrust faulting.

The integrated study resulted in inferring that the shallower gas upthrust features have a deeper origin of up to Paleocene age. The study indicates that the typical topography, subsurface configuration and geology of the study area are the resultant of the gas upthrusts, gas/fluid migration, shale diapirism and/or neotectonic activity. The deep structural and tectonic configuration in the KG offshore probably influences the distribution of gas hydrate deposits.

Acknowledgments: We wish to thank Director, National Institute of Oceanography, Goa for granting necessary permission to publish this manuscript. We sincerely thank DGH for providing the necessary data. We are grateful to the two anonymous reviewers for their constructive comments which improved our manuscript considerably. This is NIO's Contribution NO.....

References:

- Anitha, G., Ramana, M.V., Ramprasad, T., Dewangan, P., Anuradha, M., 2014. Shallow geological environment of Krishna–Godavari offshore, eastern continental margin of India as inferred from the interpretation of high resolution sparker data. *Journal of Earth System Sciences*, Indian Academy of Sciences, 123, 2, 329-342.
- Bastia, R., 2007. *Geologic Settings and Petroleum Systems of India's East Coast Offshore Basins: Concepts and Applications*. Technology Publication, Dehradun, India.
- Bastia, R., Nayak, P., 2006. Tectonostratigraphy and depositional patterns in Krishna offshore basin, Bay of Bengal. *The Leading Edge* 25, 839-845.
- Bastia, R., Singh, P., Nayak, P., 2006. Linking shelf delta to deep water: Krishna- Godavari Basin. *Journal of the Geological Society of India* 167, 618-628.

- Chatterjee, R., Mukhopadhyay, M., Paul, S., 2010. Overpressure zone under the Krishna–Godavari offshore basin: geophysical implications for natural hazard in deeper-water drilling, *Natural Hazards* doi 10.1007/s11069-010-9659-6.
- Choudhuri, M., Guha, D., Dutta, A., Sinha, S. Sinha, N., 2010. Spatiotemporal variations and kinematics of shale mobility in the K-G Basin, India. In: L. Wood, (Ed.) *Shale tectonics*, AAPG Memoir, 93, 91-109.
- Collett, T.S., Riedel, M., Cochran, J.R., Boswell, R., Presley, J., Sibal, V., Kumar, P., Sathe, A., Sethi, A., Lall, M et al., 2008. Results of the Indian National Gas hydrate Program Expedition 01 Initial reports, Directorate General of Hydrocarbons, Ministry of Petroleum and Natural Gas, New Delhi.
- Curry, J.R., Emmel, F.J., Moore, D.G., Raitt, R.W., 1982. Structure, tectonics and geological history of the Northeastern Indian Ocean. In: Nairn, A.E., Stehli, F.G. (Eds.), *The Ocean basins and margins*, Plenum, New York, vol. 6, pp. 399-450.
- Dallimore, S.R., Collett, T.S., 2005. Scientific Results from the Mallik 2002 Gas Hydrate Production Research Well Program, Mackenzie Delta, Northwest Territories, Canada. *Bull. Geol. Surv. Canada*, 585.
- Dewangan, P., Ramprasad, T., Ramana, M.V., Mazumdar, A., Desa, M., Badesab, F.K., 2010. Seabed morphology and gas venting features in the continental slope region of Krishna-Godavari basin, Bay of Bengal: Implications in gas–hydrate exploration. *Marine and Petroleum Geology* 27, 1628-1641.
- Dewangan, P., Sriram, G., Ramprasad, T., Ramana, M.V., Jaiswal, P., 2011. Fault system and thermal regime in the vicinity of site NGHP-01-10, Krishna-Godavari basin, Bay of Bengal. *Marine and Petroleum Geology* 28, 1899-1914.
- Gupta, S.K., 2006. Basin architecture and petroleum system of Krishna Godavari basin, East coast of India. *The Leading Edge* 25, 830-837.
- Holbrook, W. S., 2001. Seismic studies of the Blake Ridge: Implications for Hydrate Distribution, Methane Expulsion, and Free Gas Dynamics. *Natural Gas Hydrates: Occurrence, Distribution, and Detection*, Geophysical Monograph 124, American Geophysical Union, 235-256.
- Hyndman, R. D., Foucher, J. P., Yamano, M., Fisher, A. et al., 1992. Deep sea bottom-simulating reflectors: Calibration of the base of the hydrate stability field as used for heat flow estimates. *Earth and Planetary Science Letters* 109, 289– 301.
- Kvenvolden, K.A., 1993. Gas hydrates as a potential energy resource-a review of their methane content. In Howell, D.G., (Ed.) *The Future of Energy Gases: U.S. Geological Survey Professional Paper 1570*, 555-561.
- Kvenvolden, K.A., 1998. A primer on the geological occurrence of gas hydrate. In Henriot, J-P., Mienert, J., (Eds.) *Gas Hydrates: Relevance to World Margin Stability and Climate Change*, Geological Society London, Special Publications, 137, 9-30.
- Mandal, R., Dewangan, P., Ramprasad, T., Kumar, B.J.P., Vishwanath, K., 2014. Effect of thermal non-equilibrium, seafloor topography and fluid advection on BSR-derived geothermal gradient. *Marine and Petroleum Geology* this volume.

- Mazumdar, A., Dewangan, P., Joao, H.M., Peketi, A., Khosla, V.R., Kocherla, M., Badesab, F.K., Joshi, R.K., Roxanne, P., Ramamurty, P.B., Karisiddaiah, S.M., Patil, D.J., Dayal, A.M., Ramprasad, T., Hawkesworth, C.J., Avanzinelli, R., 2009. Evidence of paleo-cold seep activity from the Bay of Bengal, offshore India. *Geochemistry Geophysics Geosystems* 10 (6), 15. doi:10.1029/2008GC002337.
- Mazumdar, A., Peketi, A., Dewangan, P., Kocherla, M., Joshi, R.K., Ramprasad, T., 2012. Geochemical and geological constraints on the composition of marine sediment pore fluid: Possible link to gas hydrate deposits. *Marine and Petroleum Geology* 38, 35-52.
- Murthy, K. S. R., Subrahmanyam, V., Subrahmanyam, A. S., Murty, G. P. S., Sarma, K.V.L.N.S., 2010. Land-ocean tectonics (LOTs) and the associated seismic hazard over the Eastern Continental Margin of India (ECMI). *Natural Hazards* 55, 167-175, doi 10.1007/s11069-010-9523-8.
- Nemcok, M., Sinha, S.T., Stuart, S.T., Welker, C., Choudhuri, M., Sharma, S.P., Misra, A.A., Sinha, N., Venkatraman, S., 2012. East Indian margin evolution and crustal architecture: integration of deep reflection seismic interpretation and gravity modelling. In: Mohriak, W.U., Danforth, A., et al., (Eds) *Conjugate Divergent Margins*, Geological society of London Special Publication. 369. Doi: 10.1144/SP369.6
- NIO, 1997. Gas hydrates resource map of India. NIO/SP-25/97. GAIL (India) Limited, pp. 56.
- NIO, 2001. Reprocessing of multichannel seismic data of ONGC. NIO/CON/3-2001. GAIL (India) Limited, pp. 39.
- NIO, 2003. Geoscientific investigations of shallow sediments in KG offshore, East Coast. Goa NIO/TR-13/2003. ONGC Limited, pp. 103.
- Nouze, H., Henry, P., Noble, N., Martin, V., Pascal, G., 2004. Large gas hydrate accumulations on the eastern Nankai Trough inferred from new high-resolution 2-D seismic data. *Geophysical Research Letters* 31, L13308, doi:10.1029/2004GL019848
- Pateria, M. L., Rangaraju, M. K., Raiverman, V., 1992. A note on the structure and stratigraphy of Bay of Bengal sediments. In: *Recent Geoscientific Studies in the Bay of Bengal and the Andaman Sea*. Geological Survey of India Special Publication 29, 21-23.
- Raju, D.S.N., Ravindran, C.N., Mishra, P.K., Chidambaram, L, Saxena, R.K., 1994. Stratigraphy and Paleoenvironments of the Godavari clay in the Krishna-Godavari Basin, India. *Indian Journal of Petroleum Geology* 3(2), 33-43.
- Ramana, M.V., Nair, R.R., Sarma, K.V.L.N.S., Ramprasad, T., Krishna, K.S., Subrahmanyam, V., Maria, D'Cruz., Subrahmanyam, C., Paul, J., Subrahmanyam, A.S., Chandra Sekhar, D.V., 1994. Mesozoic anomalies in the Bay of Bengal. *Earth Planetary Science Letters* 121, 469-475.
- Ramana, M.V., Ramprasad, T., Desa, M., Sathe, A.V., Sethi, A.K., 2006. Gas hydrates-related proxies inferred from multidisciplinary investigations in the Indian offshore areas. *Current Science* 91(2), 183-189.
- Ramana, M.V., Ramprasad, T., Paropkari, A.L., Borole, D.V., Ramalingeswara Rao, B., Karisiddaiah, S.M., Desa, M., Kocherla, M., Joao, H.M., Loka-bharathi, P., Gonsalves, Maria-Judith, Pattan, J.N., Khadge, N.H., Prakash Babu, C., Sathe, A.V., Kumar, P., Sethi, A.K.,

2009. Multidisciplinary investigations exploring indicators of gas hydrates occurrence in the Krishna-Godavari basin offshore, east coast of India. *Geo-Marine Letters* 29 (1), 25-38.
- Ramprasad, T., Dewangan, P., Ramana, M.V., Mazumdar, A., Karisiddaiah, S.M., Ramya, E.R., Sriram, G., 2011. Evidence of slumping/sliding in Krishna Godavari offshore basin due to gas/fluid movements. *Marine and Petroleum Geology* 28, 1806-1816.
- Rao, G.N., 2001. Sedimentation, stratigraphy, and petroleum potential of Krishna–Godavari basin, East coast of India. *Bull. American Association of Petroleum Geologists Bulletin* 85 (9), 1623-1643.
- Rao, G.N., Mani, K.S., 1993. A study on generation of abnormal pressures in Krishna-Godavari Basin, India. *Indian Journal of Petroleum Geology* 2 (1), 20-30.
- Riedel, M., Collett, T.S., Kumar, P., Sathe, A.V., Cook, A., 2010. Seismic imaging of a fractured gas hydrate system in the Krishna–Godavari Basin, offshore India. *Marine and Petroleum Geology* 01/2010; DOI:10.1016/j.marpetgeo.2010.06.002
- Riedel, M., Collett, T.S., Shankar, U., 2011. Documenting channel features associated with gas hydrates in the Krishna–Godavari Basin, offshore India. *Marine Geology* 279, 1-11.
- Sahu, J.N., 2005. Deep water Krishna–Godavari basin and its potential, *Petromin (Asia’s Exploration and Production Business magazine)*, April issue, pp. 26-34.
- Sastri, V. V., Venkatachala, B. S., Narayana, V., 1981. The evolution of the east coast of India, *Palaeogeography, Palaeoclimatology, Palaeoecology*, 36, 23-53.
- Satyanarayana, K., Rao, G.N., Bhavana, P.R., Sinha, H.R., Banerjee, A.N., 1996. Miocene sedimentation in subsurface of Godavari Delta. *Bulletin of Oil and Natural Gas Commission* 33(1), 77-92.
- Shanmugam, G., 2009. Slides, Slumps, Debris Flows and Turbidity Currents. In: Steele, J. H., Turekian, K.K., Thorpe, S.A. (Eds.), *Encyclopaedia of Ocean Sciences*, Second edition. Elsevier, pp. 447- 467.
- Shanmugam, G., Shrivastava, S.K., Das, B., 2009. Sandy Debrites and Tidalites of Pliocene Reservoir Sands in Upper-Slope Canyon Environments, Offshore Krishna–Godavari Basin (India): Implications, *Journal of Sedimentary Research* 79(9), 736-756.
- Shipley, T.H., Houston, M.H., Buffler, R.T., Shaub, F.J., McMillen, K.J., Ladd, J.W., Worzel, J.L., 1979. Seismic reflection evidence for the widespread occurrence of possible gas-hydrate horizons on continental slopes and rises. *American Association of Petroleum Geologists Bulletin* 63, 2204-2213.
- Sloan, E.D., 1990. *Clathrate Hydrates of Natural Gases*, Marcel Dekker, Inc., New York. pp. 641.
- Suess, E., Torres, M.E., Bohrmann, G., Collier, R.W., Rickert, D., Goldfinger, C., Linke, P., Heuser, A., Sahling, H., Heeschen, K., Jung, C., Nakamura, K., Greinert, J., Pfannkuche, O., Trehu, A., Klinkhammer, G., Whiticar, M.J., Eisenhauer, A., Teichert, B., Elvert, M., 2001. Sea floor methane hydrates at Hydrate Ridge, Cascadia margin. In: Paull, C.K., Dillon, W.P. (Eds.), *Natural Gas Hydrates: Occurrence, Distribution and Detection*. Geophysical Monograph, 124, 87–98.

Figure Captions

- Figure 1: Map showing the structure and tectonic frame work of KG Basin, East Coast of India. The Krishna and Godavari are the two major perennial rivers flowing into the Bay of Bengal in the study area. The onshore is dominated by NE-SW trending horst and grabens. The Eocene Shelf Edge, Paleogene and Neogene growth faults, toe thrust fault and shale diapirism are some of the characteristic features of the KG offshore (Rao and Mani, 1993; Rao, 2001; Bastia, 2006). Inset shows location of the KG Basin on the East Coast of India.
- Figure 2: Map showing the tracks of the different data types used in the present study. The thin black lines depict the high resolution seismic reflection (HRS) data acquired using 10 KJ Sparker System. Blue and red lines represent the tracks of the multichannel seismic (MCS) data. Figure numbers of the detailed sections are indicated. General bathymetry is shown as thin outlines at 500m contour interval. Inset shows location of the KG Basin on the East Coast of India. NGHP-01 well locations are shown as red dots. The green dot is the location of the oil industry deep drill well used in the study for stratigraphy.
- Figure 3: Processed and interpreted HRS sections along the tracks (a) L1, (b) L2, (c) L3, (d) L4, (e) L5, (f) L6, (g) L7, (h) L8, (i) L9. The location of these tracks is shown in figure 2. Dashed lines indicate faults and/or gas/fluid pathways. LGM: Last Glacial Maximum, GU: Gas Upthrust, CGS: Columnar type Gas saturated zone/vent, TF: toe thrust fault, MTD: Mass Transport Deposits, ATZ: Acoustically Transparent Zone. The location of these tracks is shown in figure 2.
- Figure 4: Processed and interpreted multichannel seismic sections (a) AD-1 which runs along HRS line L2 (b) AD-2 running along HRS line L4, and (c) AD-3 running along HRS line L8. The sections depict the seismic sequences from Eocene to Recent (H3 to H6). Various features are shown as per legend. BSR: Bottom Simulating Reflector. The location of these profiles is shown in figure 2.
- Figure 5: (a) (i) High quality multichannel seismic section along the profile GXT-1. (ii) Interpreted seismic section (GXT-1) depicting the basement (red outline) and various horizons (H1 to H6) within the sedimentary column. Dashed lines are the faults, while black lines are other prominent reflectors. The well stratigraphy is shown for correlation with the inferred major horizons. (b) (i) Multichannel seismic section along the profile GXT-2 (ii) Interpreted seismic section GXT-2. Moho is shown as blue outline. Other information as in figure 5a. (c) Detailed interpretation of the slope area with major geological boundaries and series of thrust complexes (TC) along the profile GXT-1. (d) Detailed view of the delta front along line GXT-2. (e) Detailed view of slumping along line GXT-2.
- Figure 6: (a) Schematic model depicting the various stages of deposition of the sedimentary column in the KG offshore. Black dashed lines represent faults, while red dashed outline depicts gas upthrust (GU)/diapirism. B1 and B2 indicate bulging due to shale diapirism. TC: Series of thrust complexes.

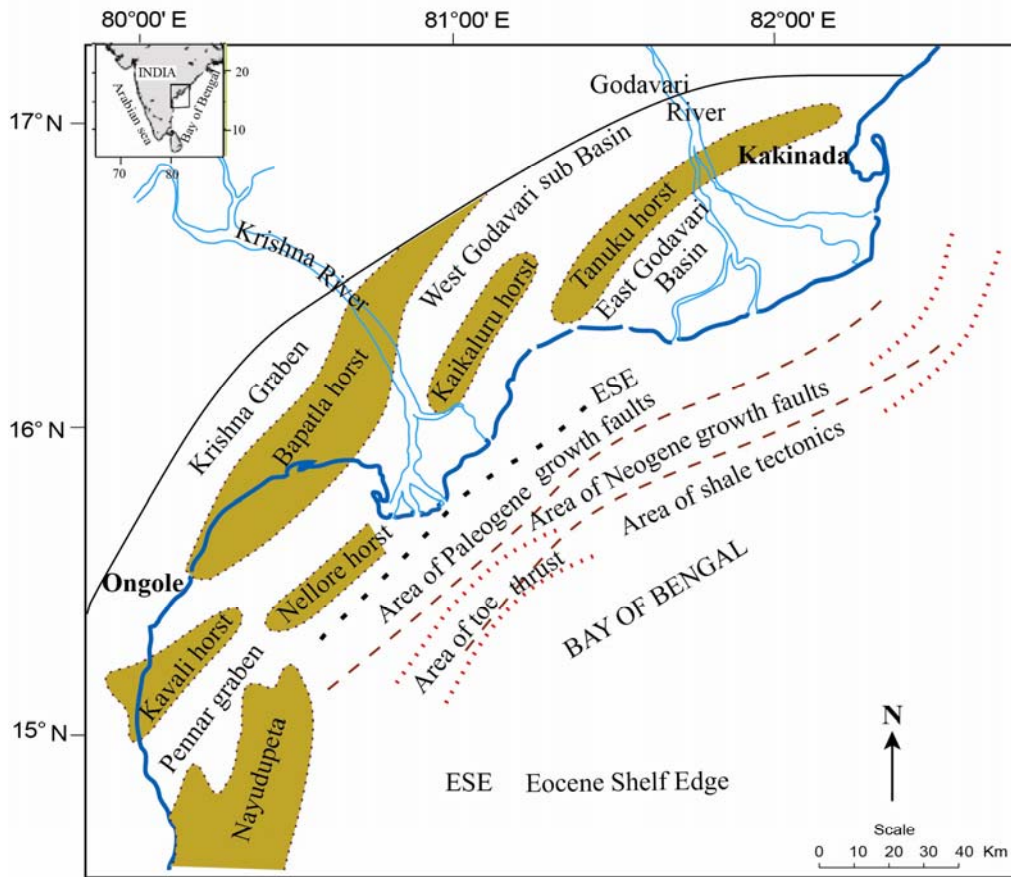


Fig.1

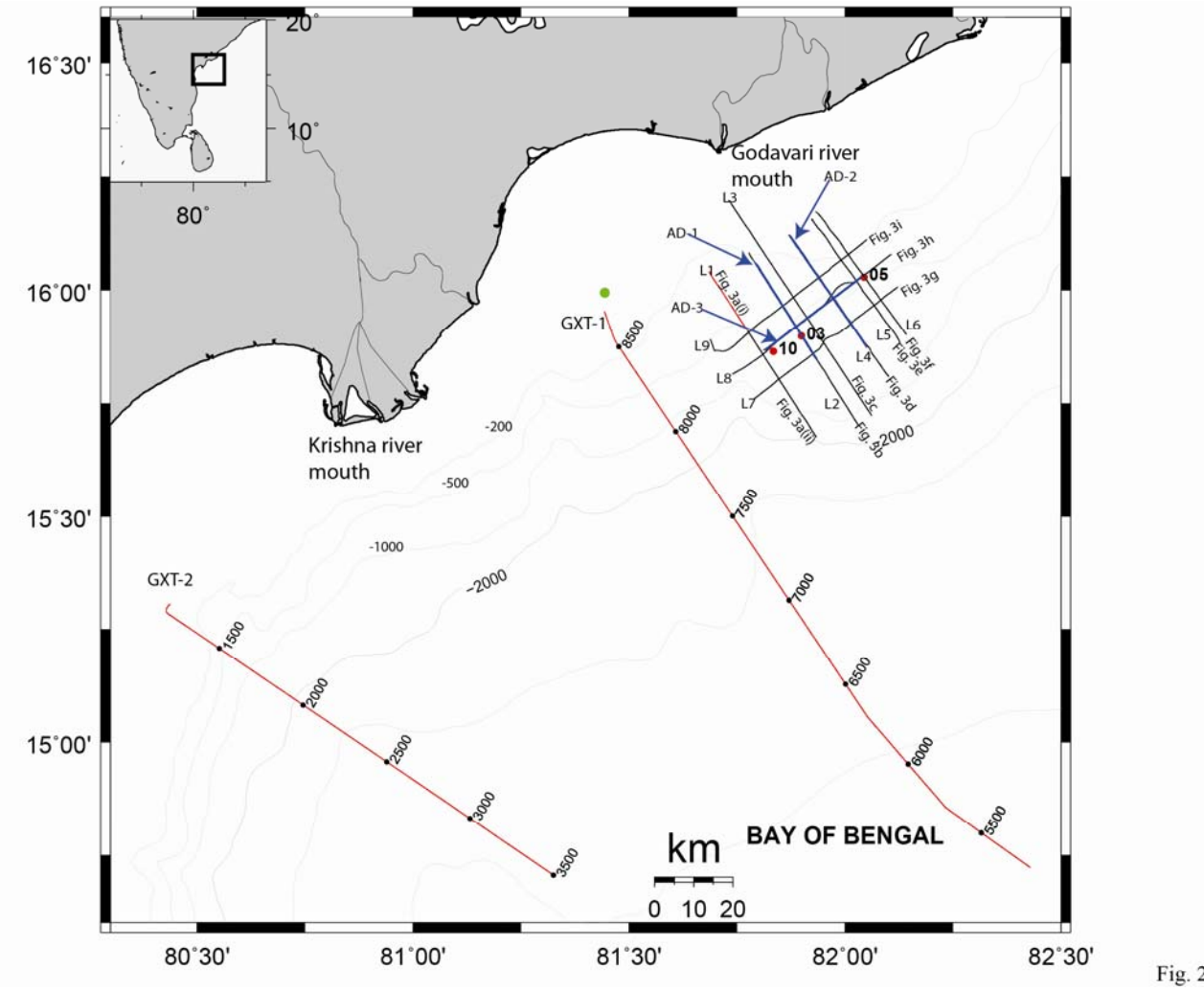


Fig. 2

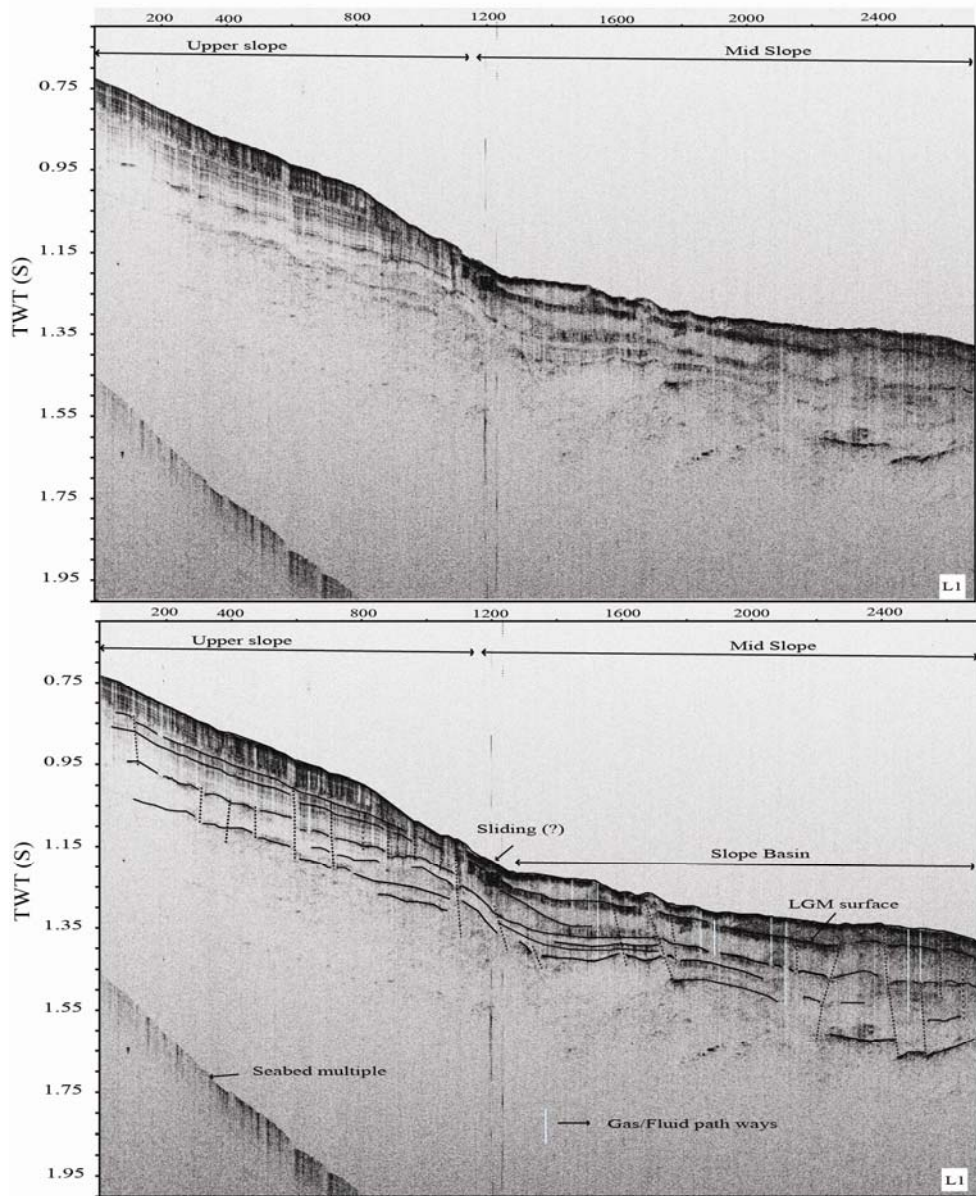


Fig.3a

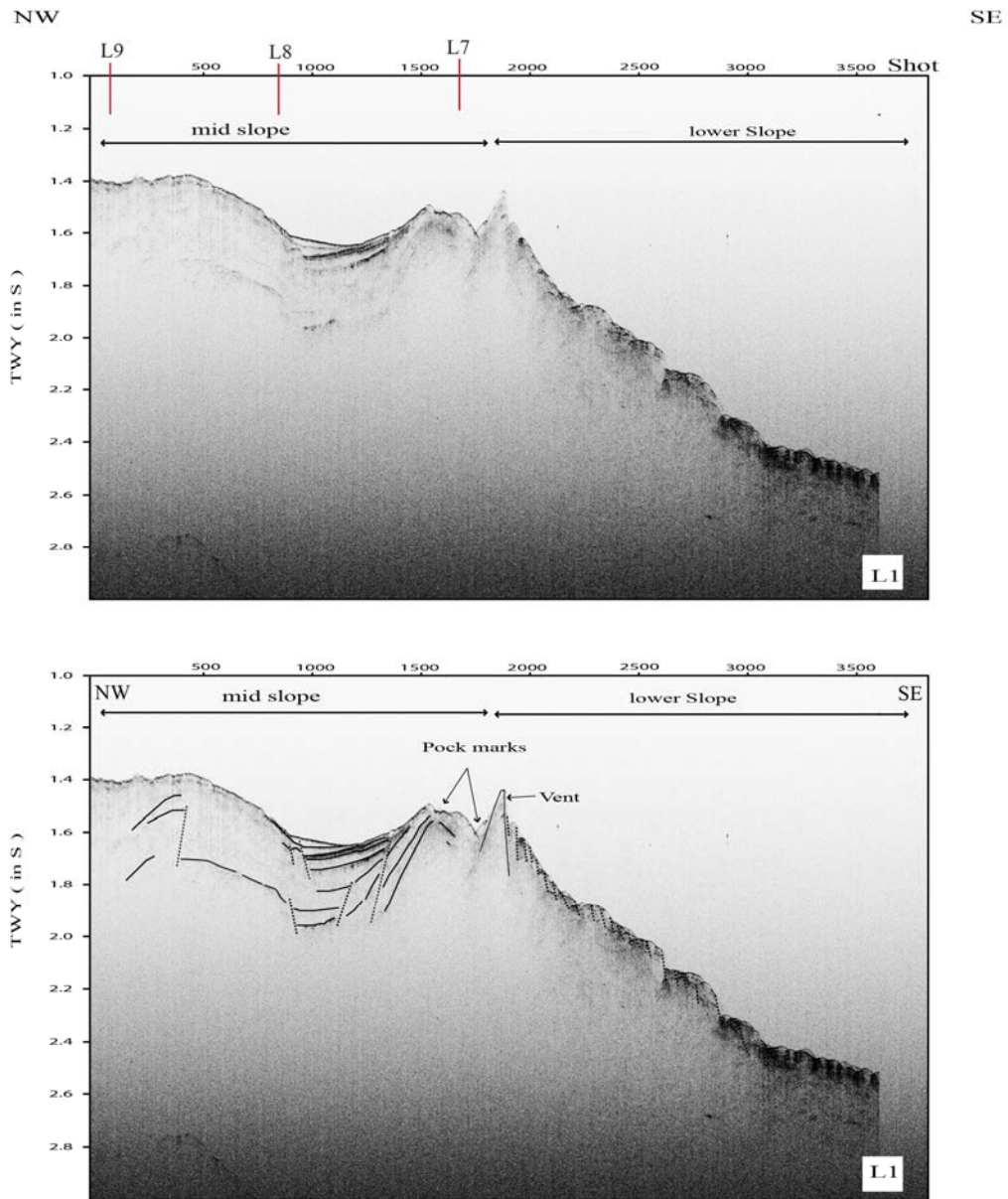


Fig. 3a

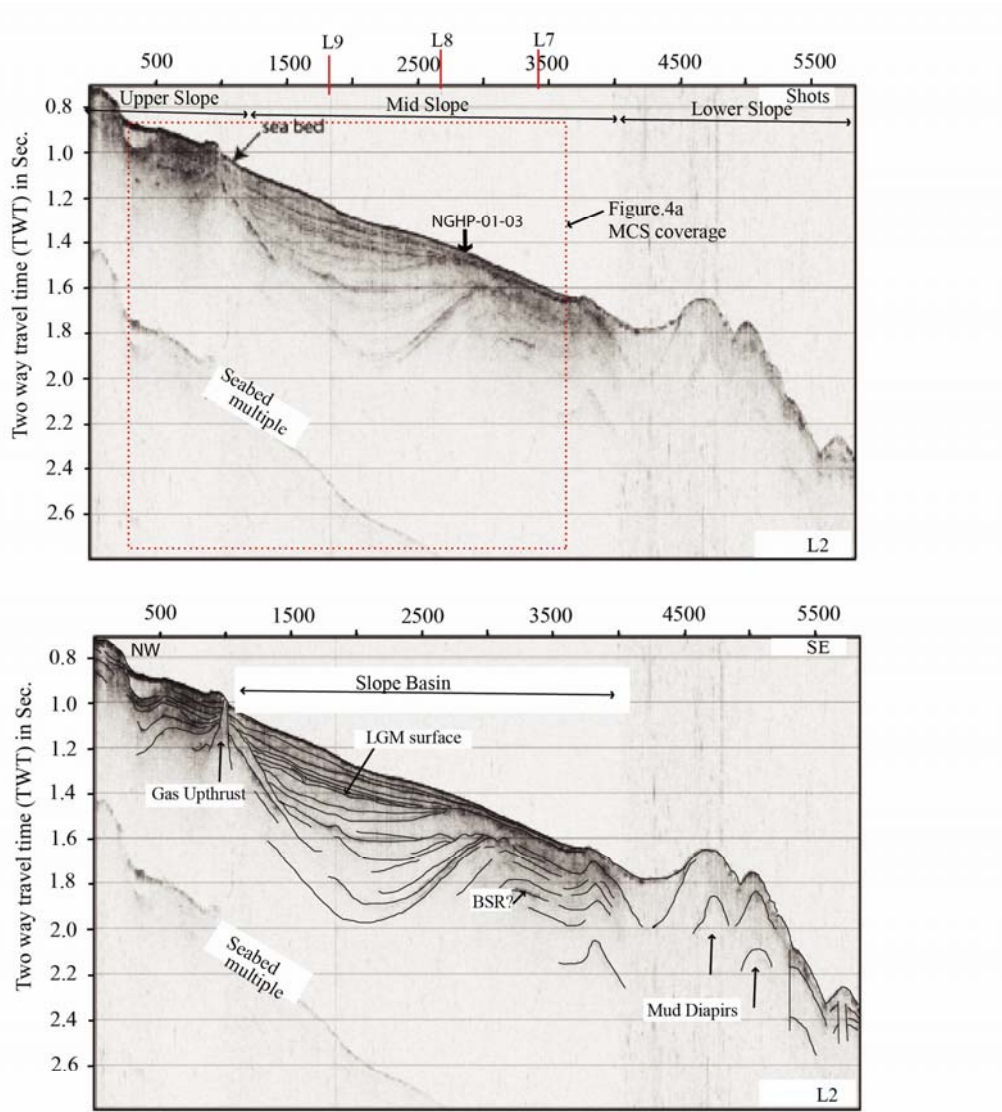


Fig. 3b

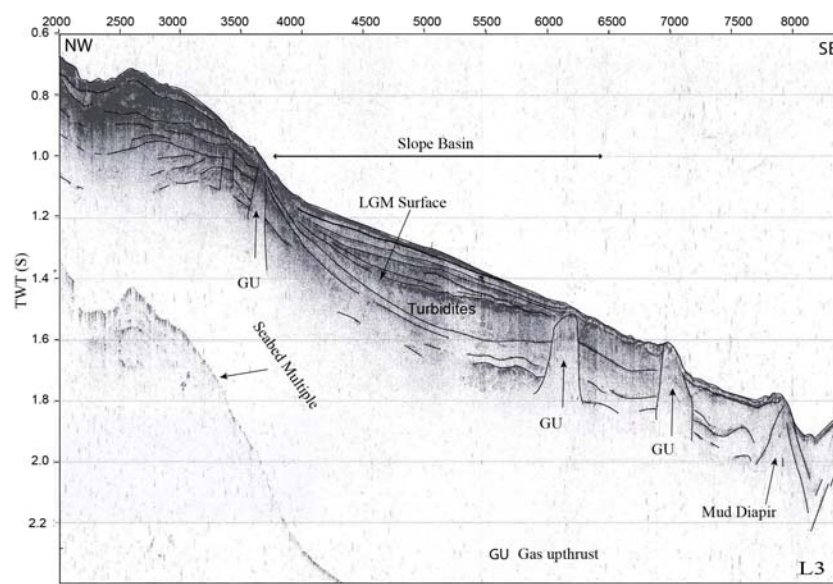
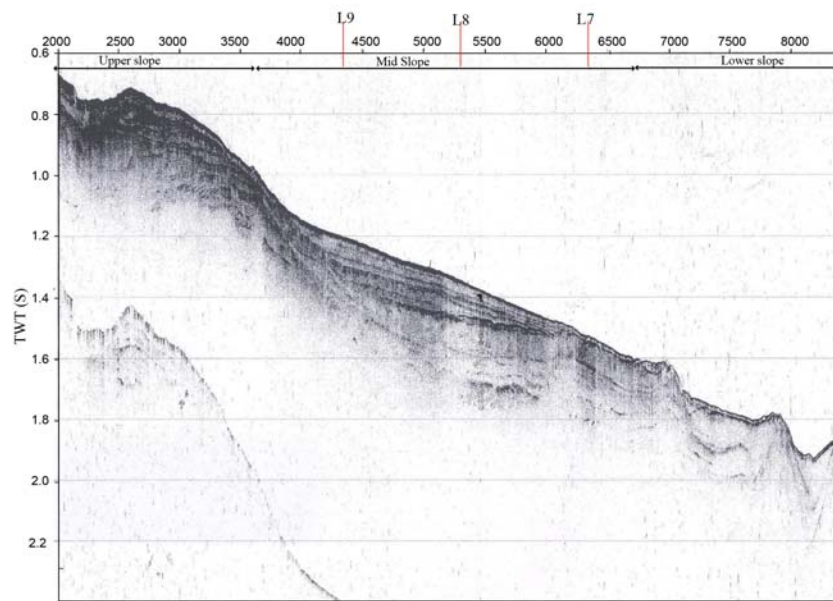


Fig. 3c

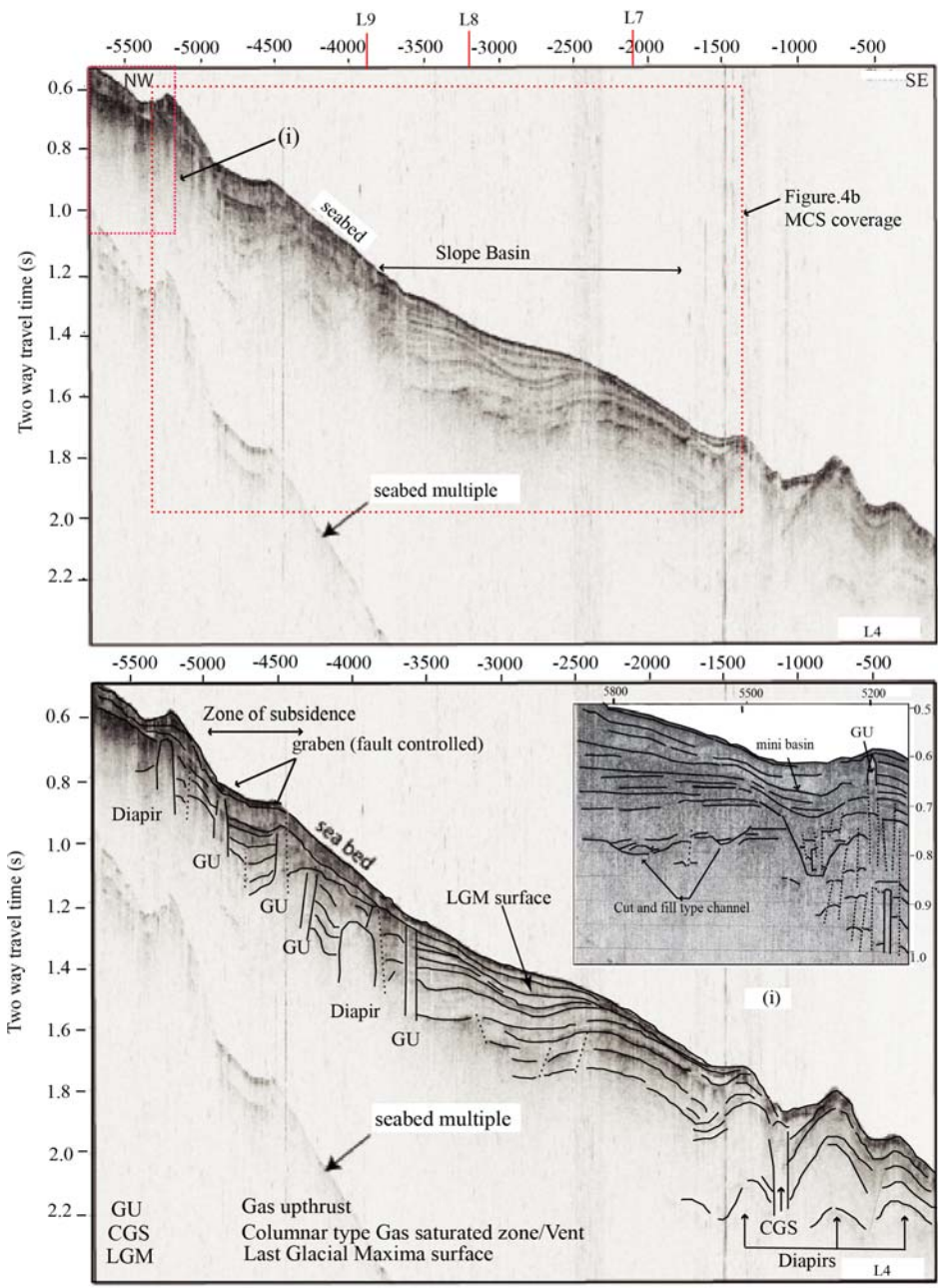


Fig. 3d

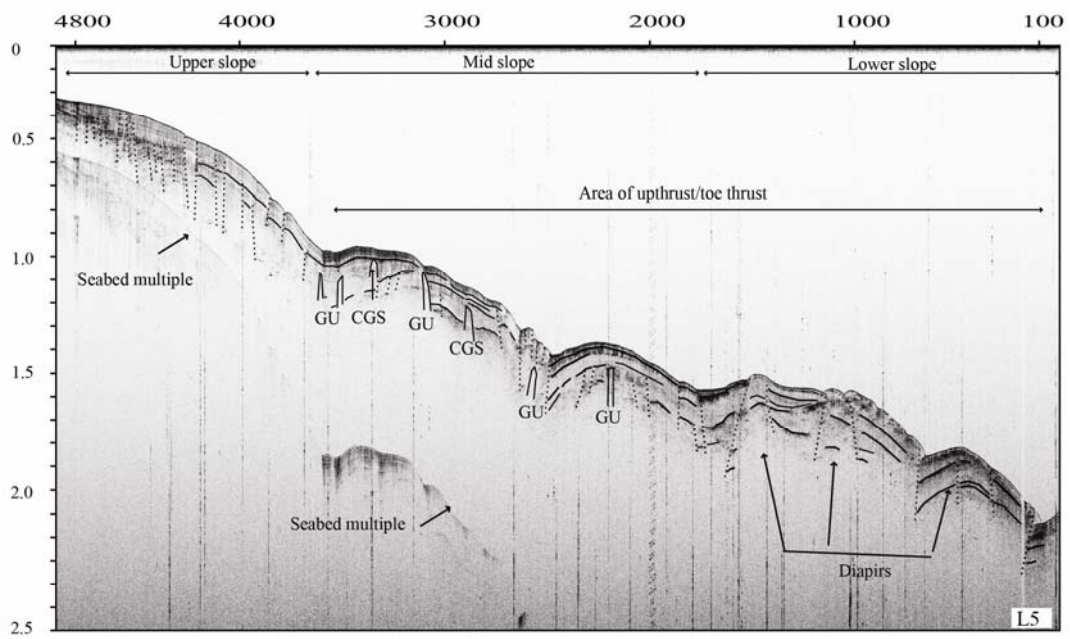
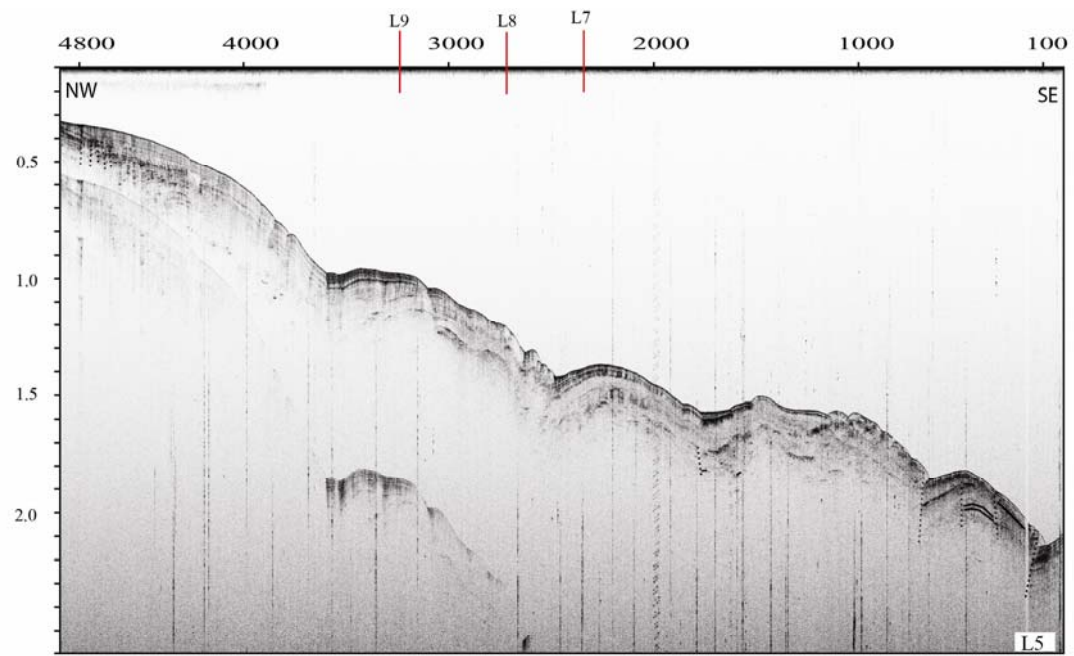


fig.3c

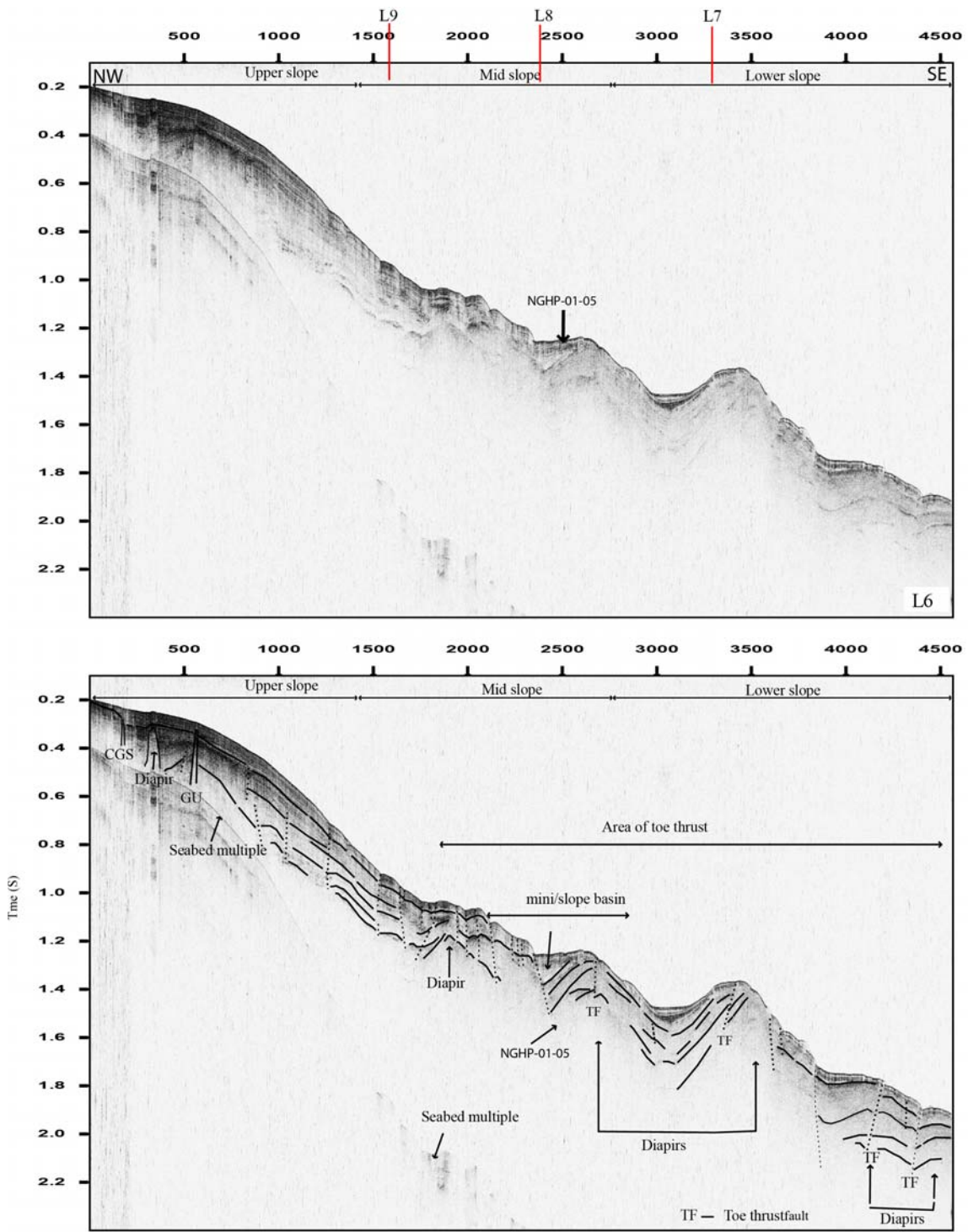


Fig.3f

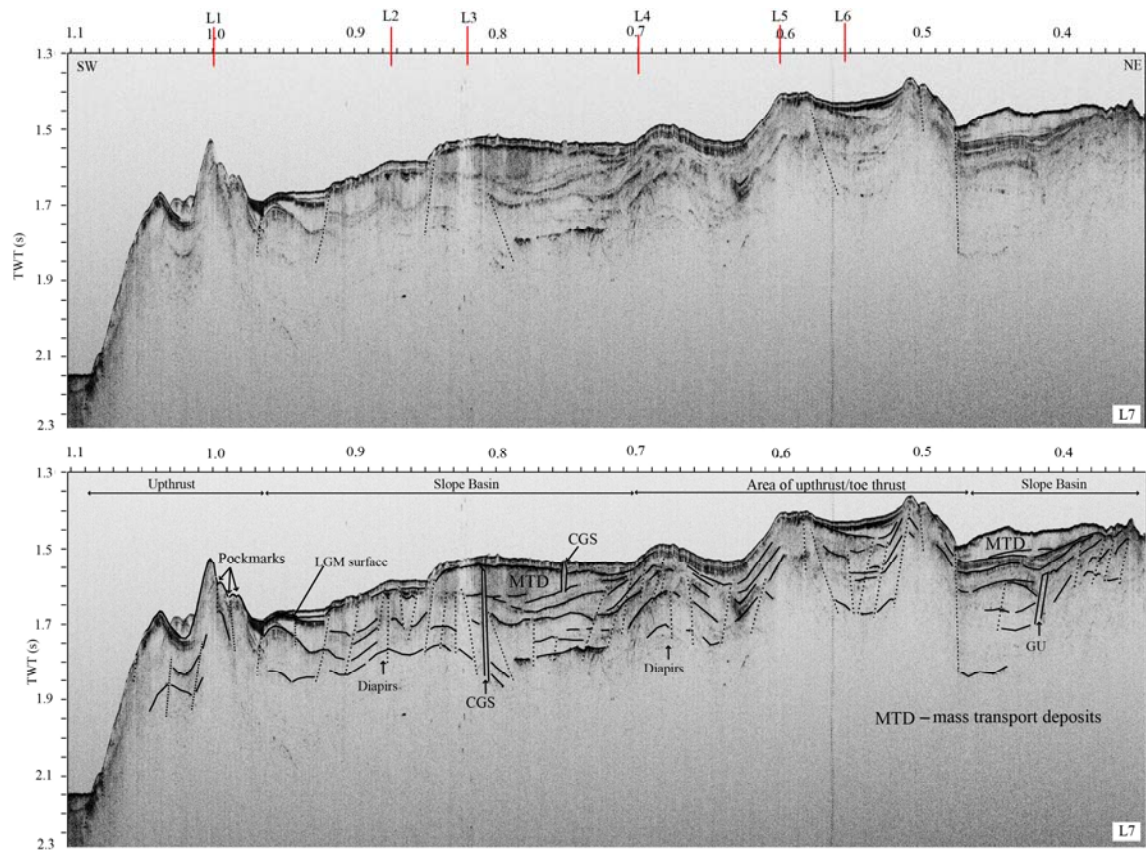


Fig.3g

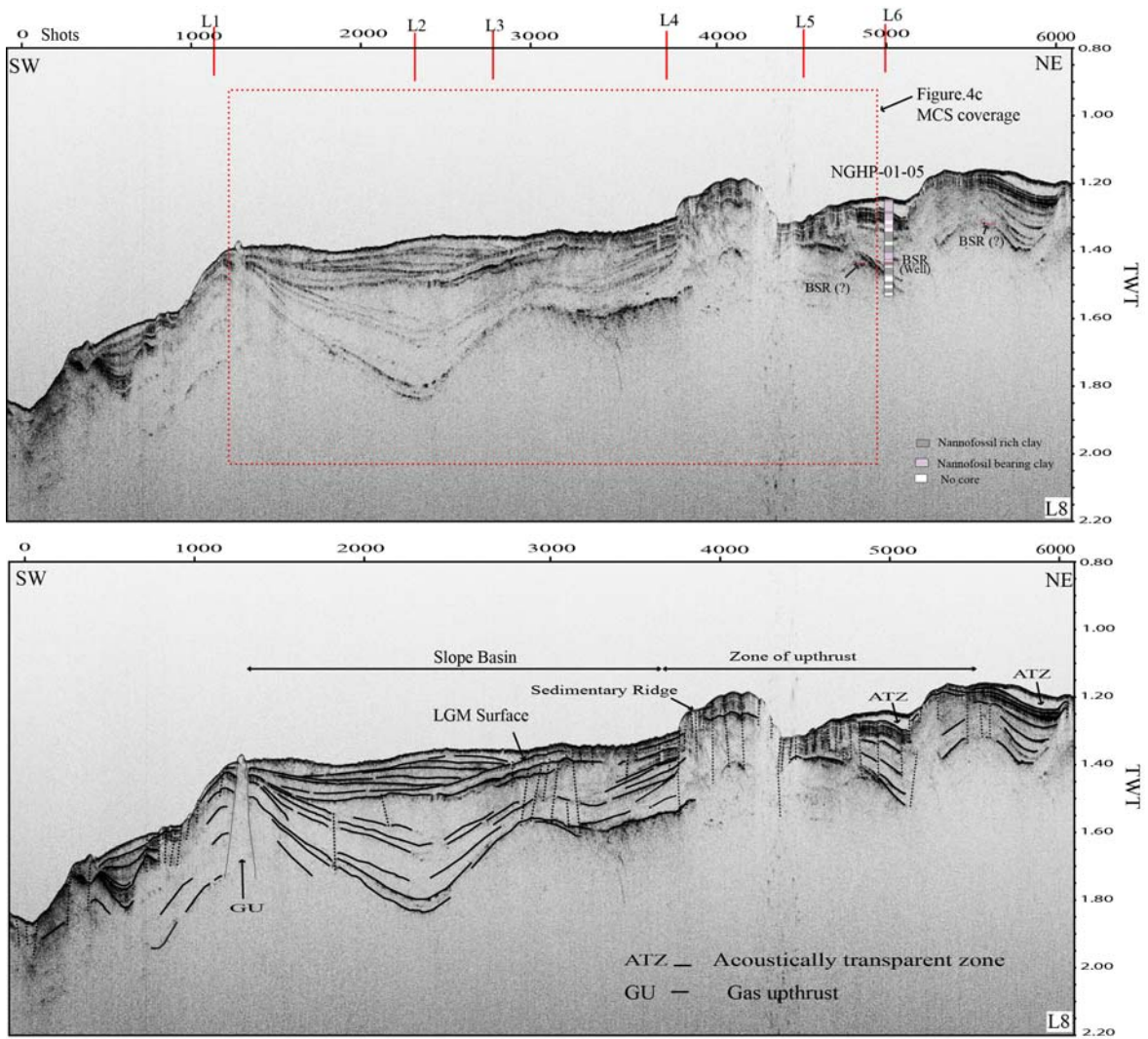


Fig.3h

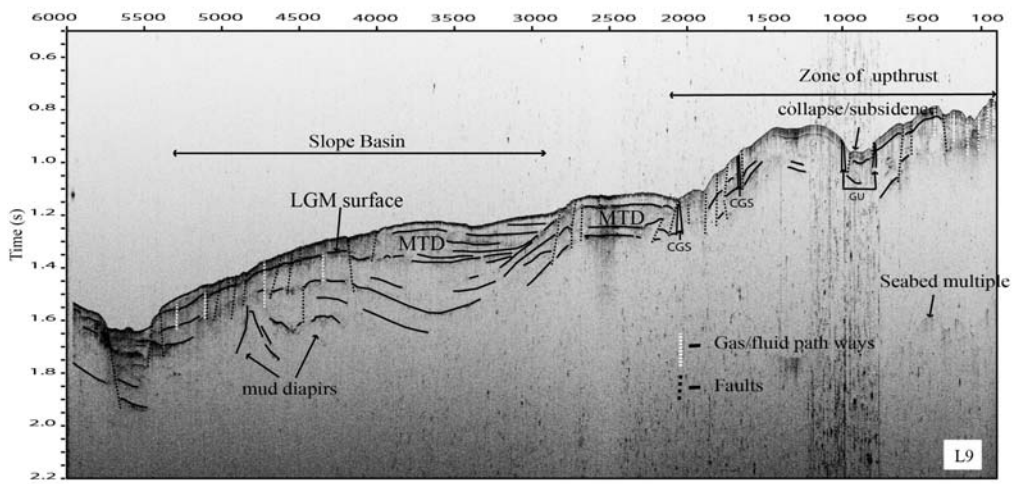
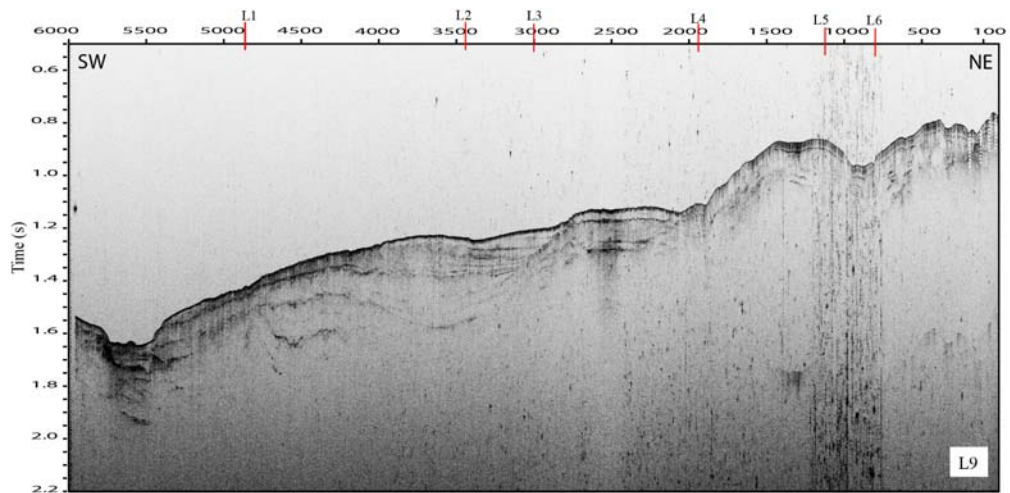


Fig.3i

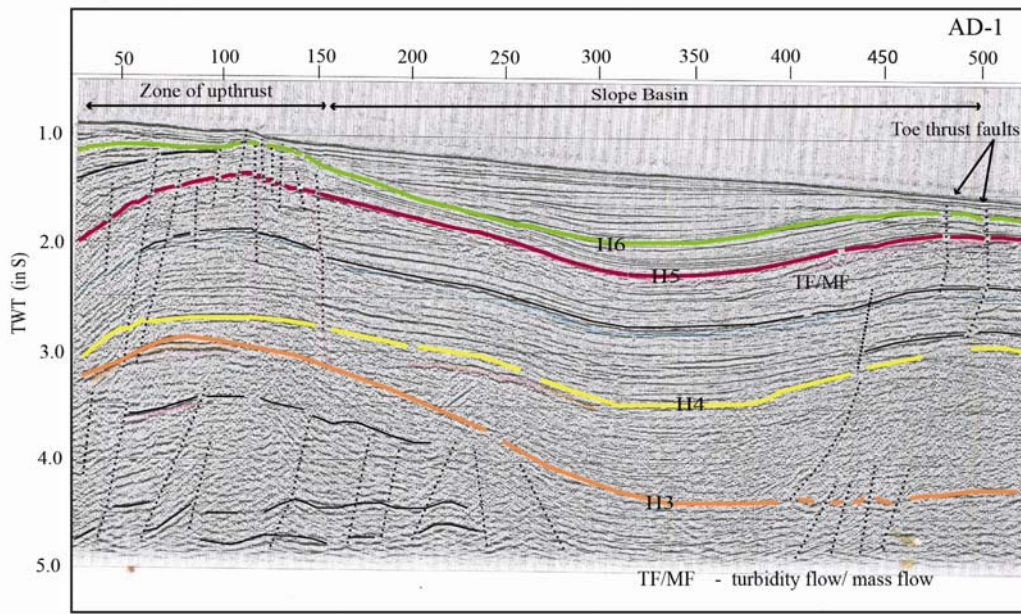
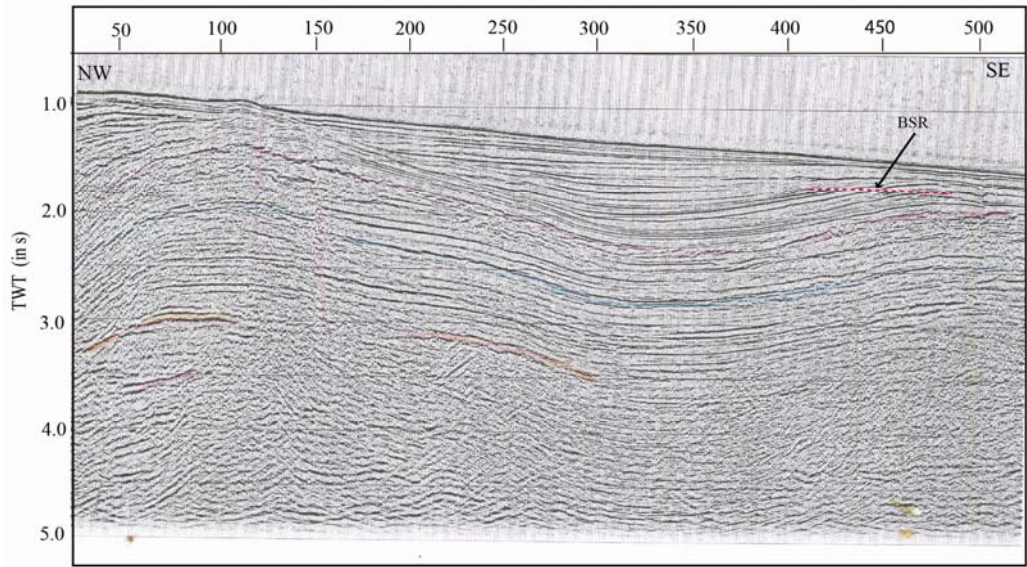
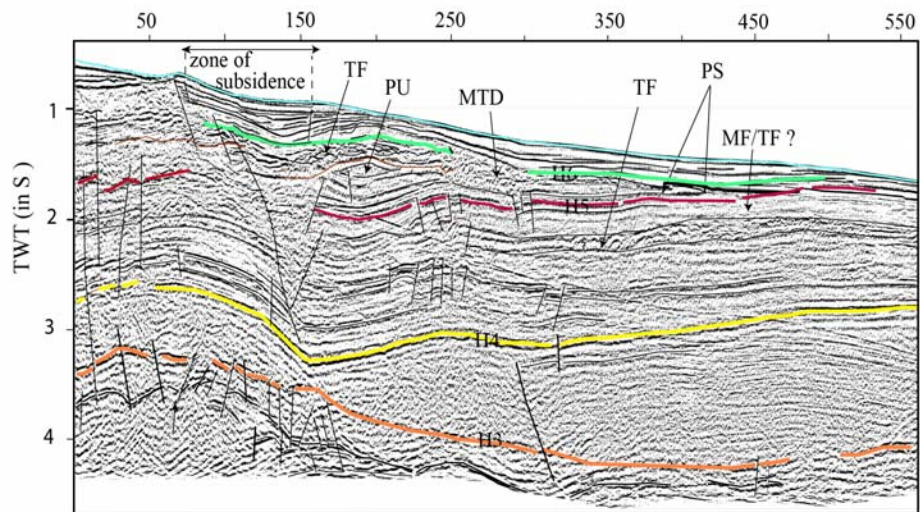
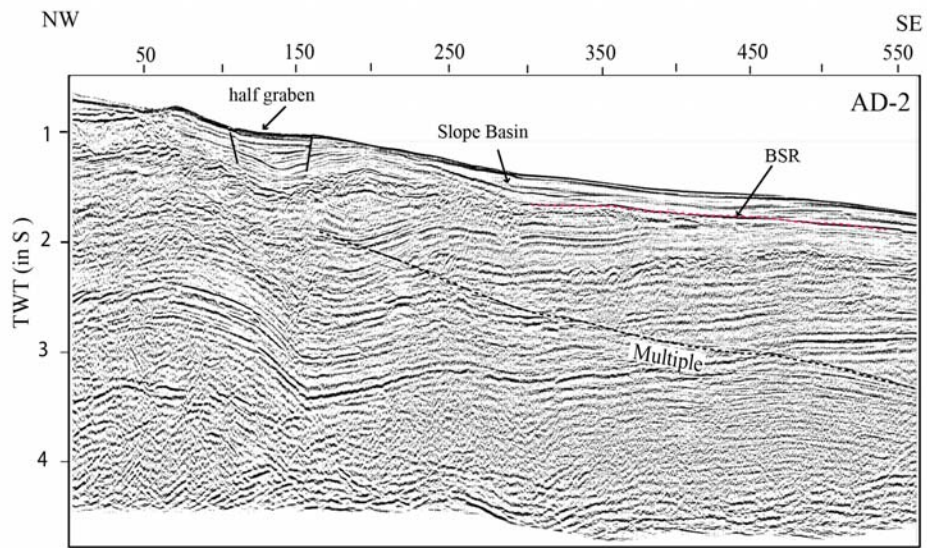


Figure.4a



LEGEND

- | | | | |
|-------|--------------------------|-----|---------------------------------------|
| TF | turbidite flow | PU | pull-up structure due to gas upthrust |
| / | faults | PS | Pinchout structure |
| MF/TF | Mass flow/turbidite flow | MTD | Mass transport deposits |

Fig. 4b

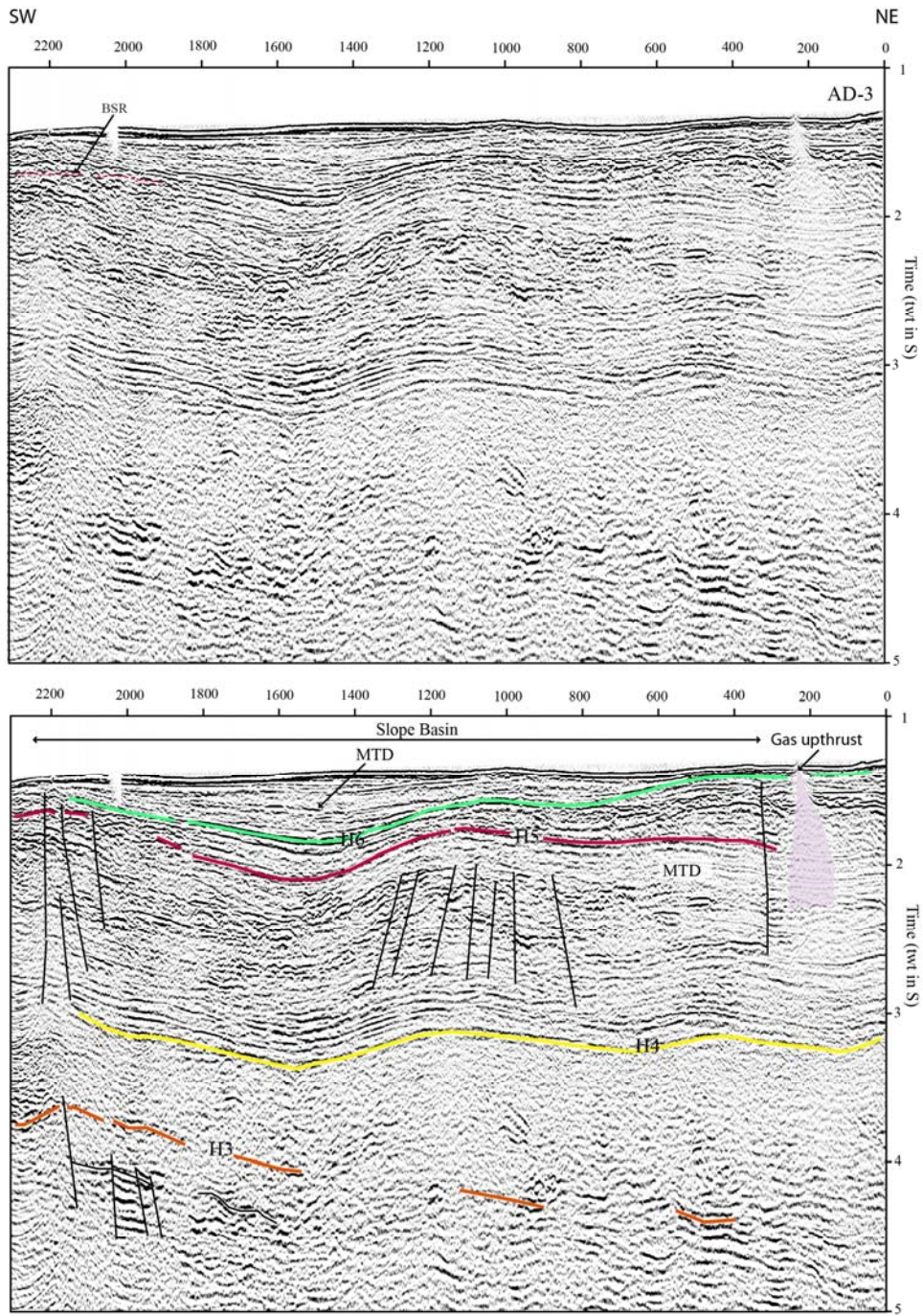
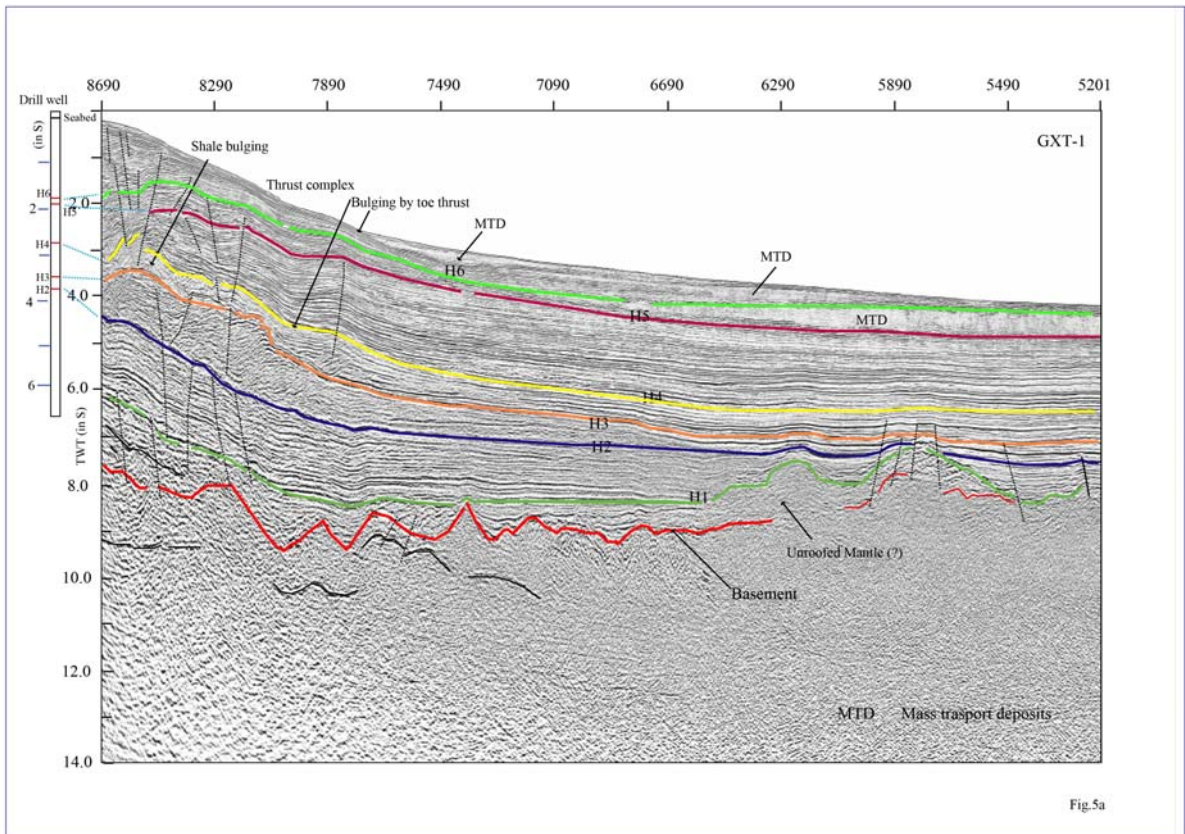
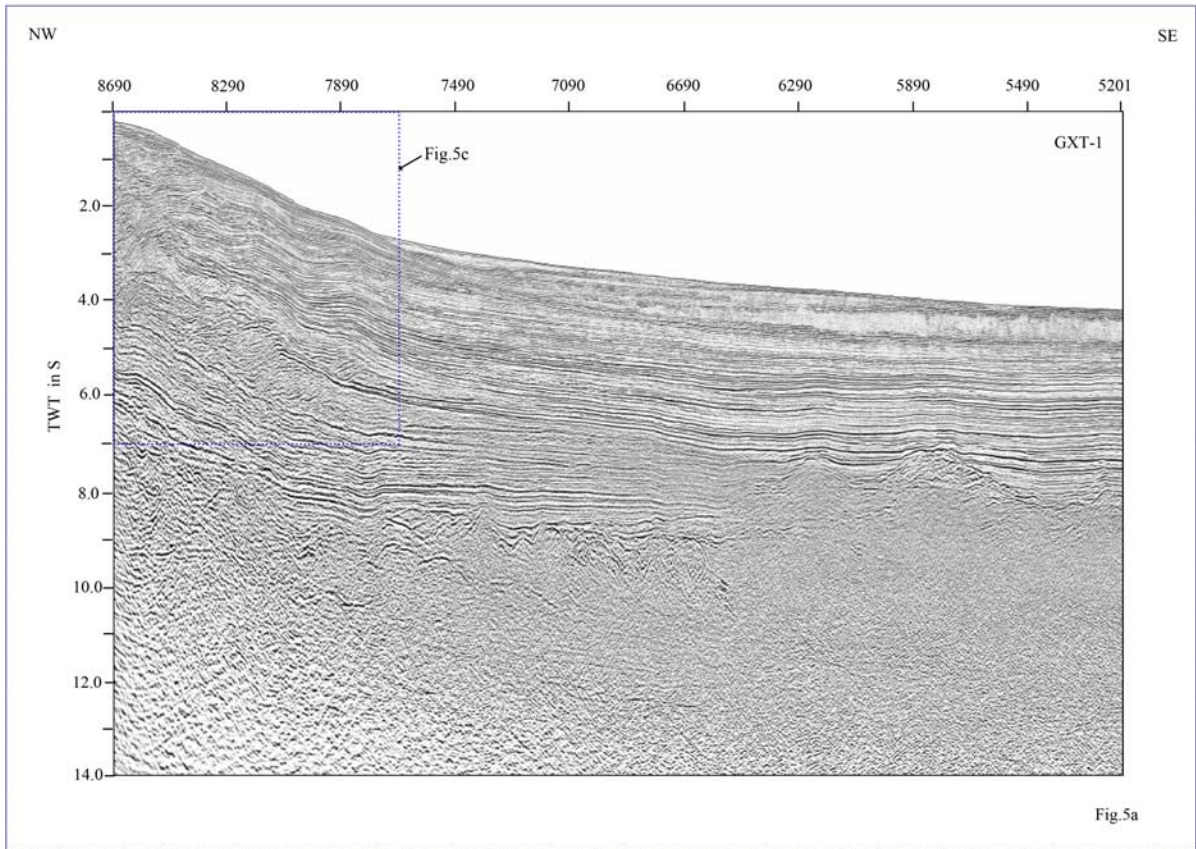


Figure.4c



i)

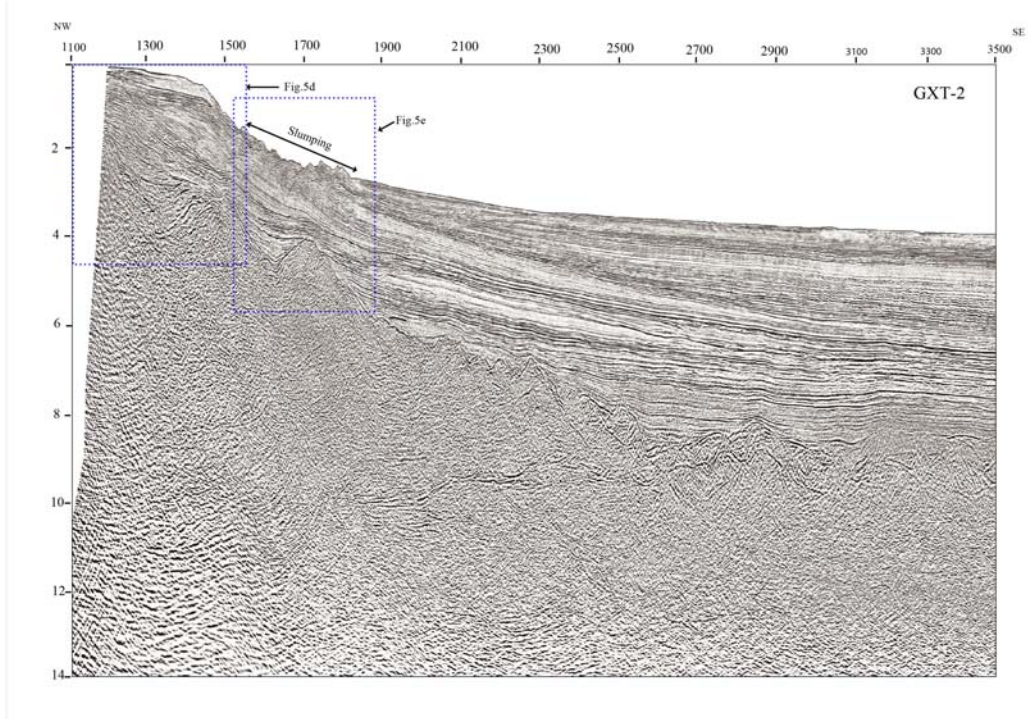


Figure 5b(i)

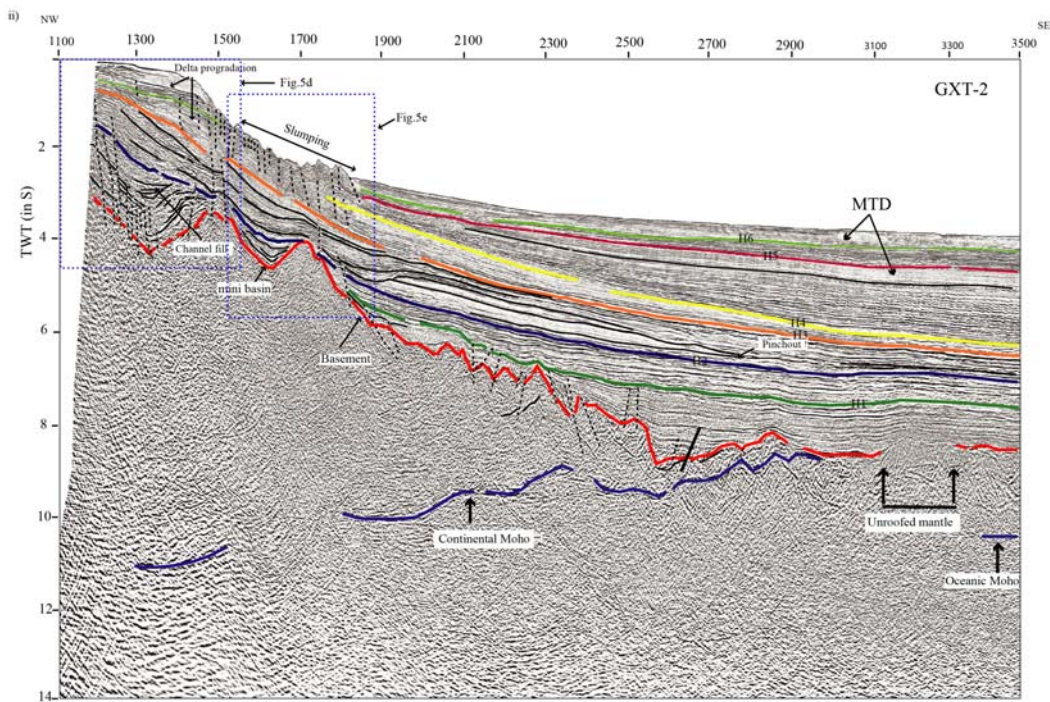


Figure 5b

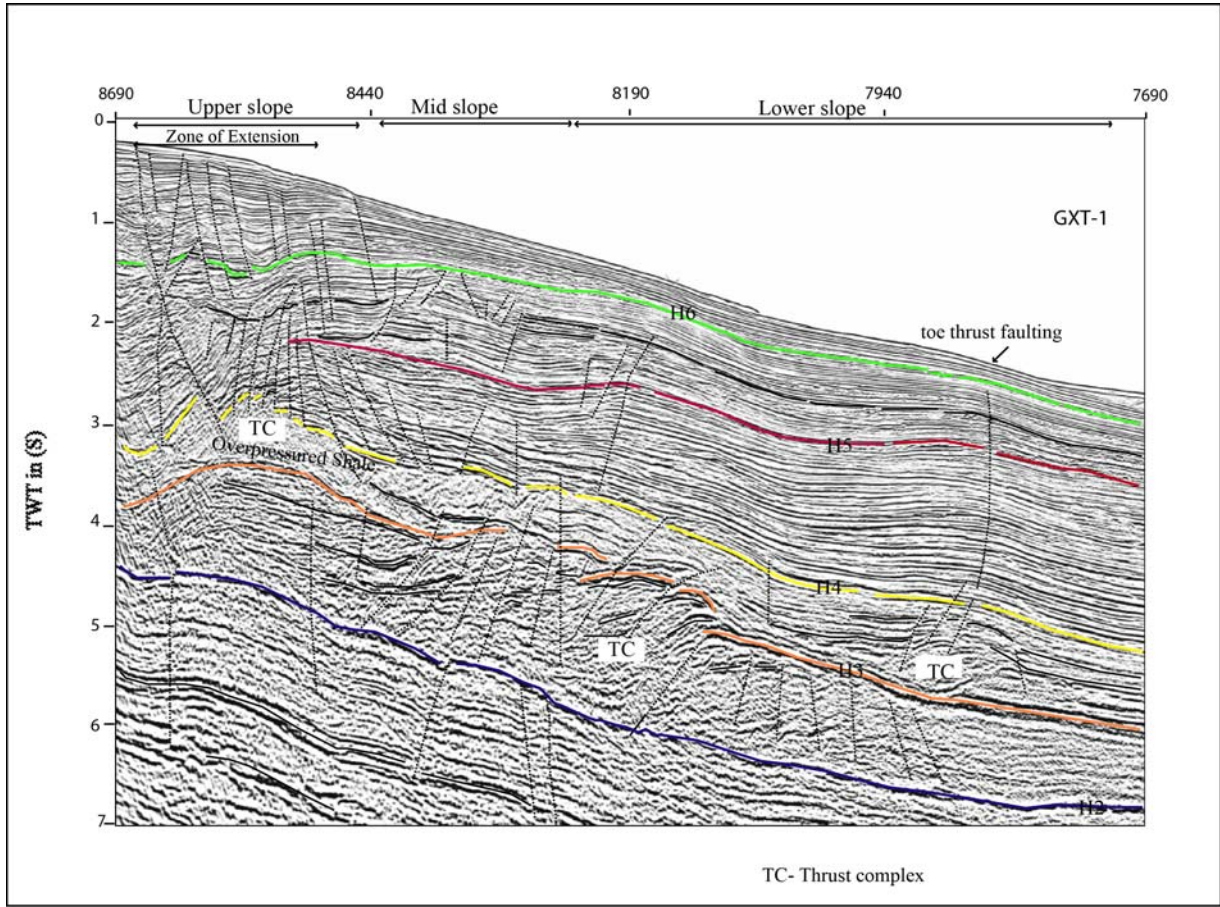


Fig.5c

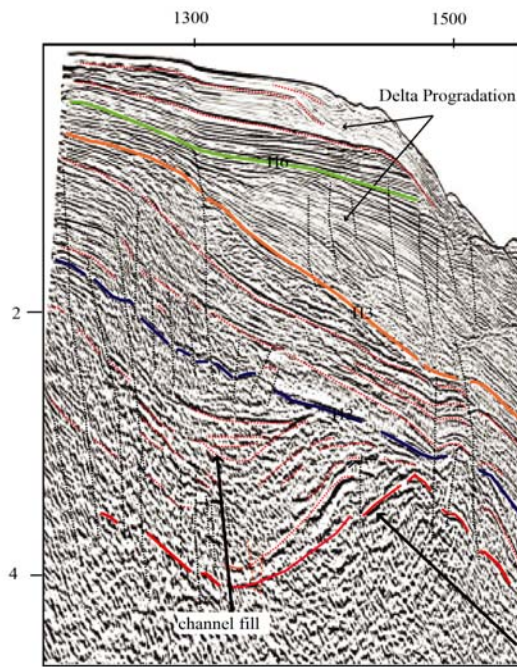


Figure 5d

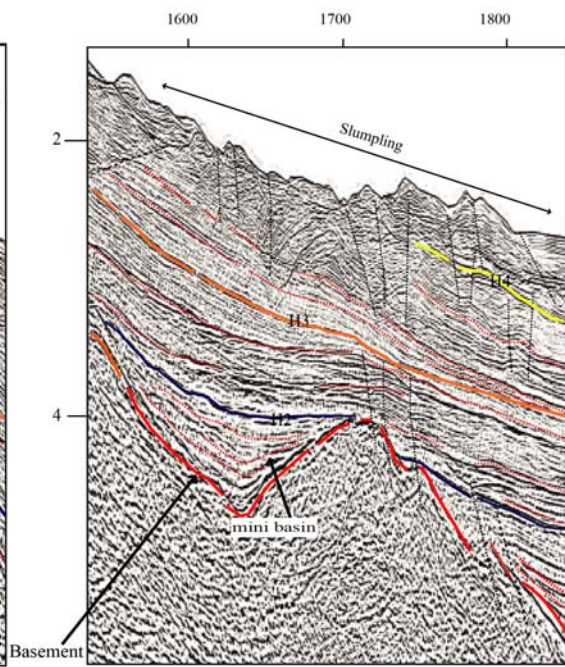


Figure 5e

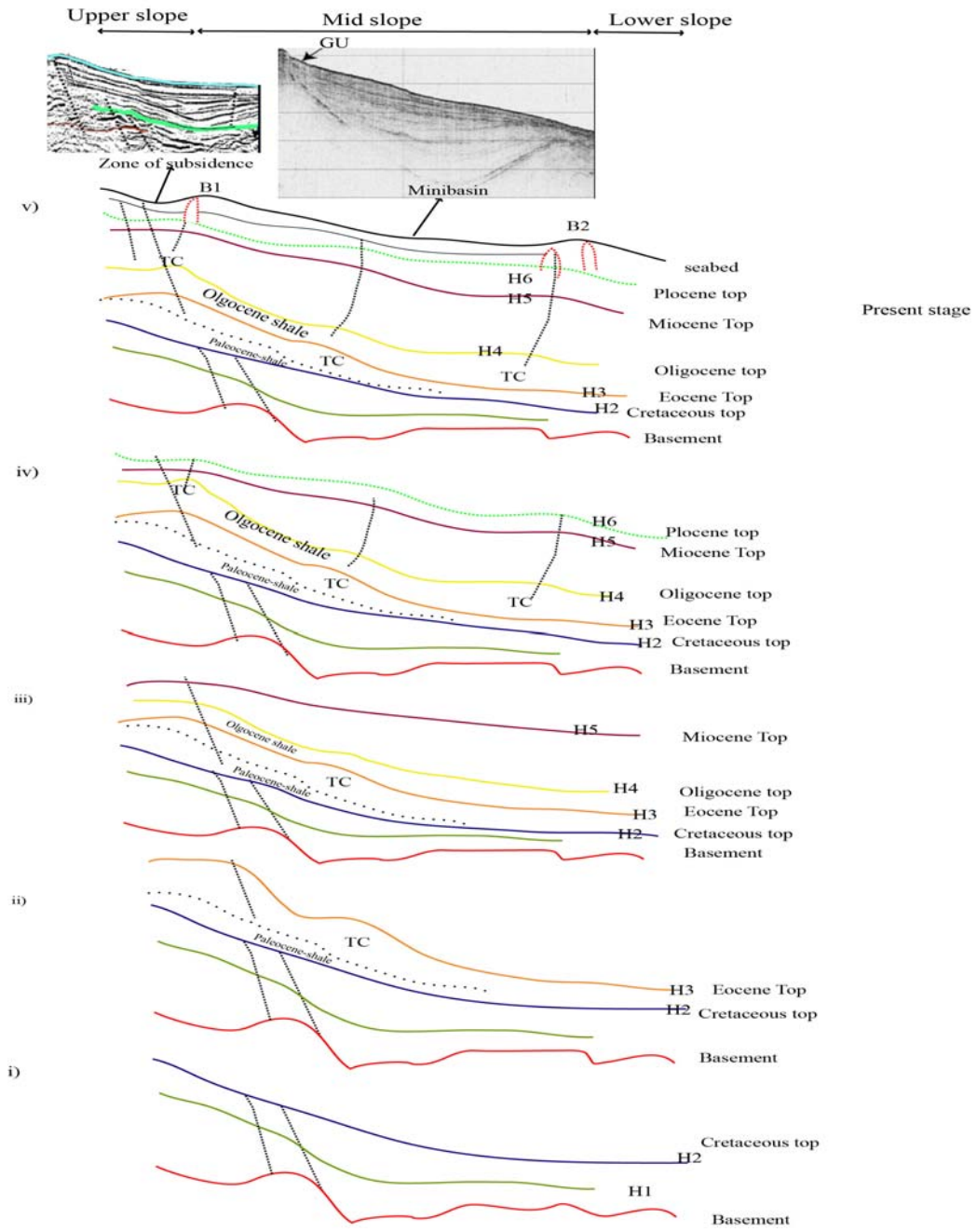


Fig.6